Polymer modified ion exchange adsorbent for the flow-through chromatography of hepatitis B virus-like particle

Ng Hon Wei

(Master of Engineering in Chemical Engineering, University of Nottingham, Malaysia Campus)

A thesis submitted for the Master of Engineering Science (Research) at Monash University in 2018
School of Engineering

Copyright Notice

Abstract

Virus-like particles (VLP) have gained attention in recent years due to its potential application in vaccine development, drug encapsulation, and targeted gene delivery. Purification of VLP with bind-and-elute mode ion exchange chromatography encounters setbacks such as low adsorption capacity and disintegration of the VLPs. Size selective flow-through chromatography (FC) can be employed to overcome these problems, where small host cell proteins (HCPs) molecules are adsorbed and the large hepatitis B core antigen virus like particles (HB-VLPs) are recovered in the flow-through fraction. In this study, a poly[oligo(ethylene glycol) methacrylate] (POEGMA) grafted adsorbents were developed to reduce the adsorption of HB-VLPs. The effect of feedstock conditions (size of target protein and protein load) and adsorbent design (adsorbent size, type of polymer chain and POEGMA architecture) on the performance of FC were investigated. The feedstock containing hepatitis B core antigen-Y132 tridimers (HB-tridimers) - a much smaller variant of the HB-VLPs, was employed to evaluate the effect of target protein size on the adsorption capacity of the adsorbent. Breakthrough curves indicated that overall adsorption capacity of adsorbent was significantly reduced with feedstock containing HB-VLPs, likely due to limited diffusivity of HB-VLPs and large HCPs. The suitable range of protein load for the adsorbent was found to be at 5.5-7.0 mg total protein/ml adsorbent (approximately 15% HCPs breakthrough). The design of the adsorbents also significantly affects the adsorption of HB-VLPs. The use of larger Sepharose Q FF significantly increased flow-through recovery (approximately 2 fold) due to a reduction in surface available for adsorption of the HB-VLPs. Grafted POEGMA was shown to be more suitable for HB-VLPs exclusion compared to the grafted charged dextran, indicating that the non-charged, hydrophilic and inert properties of POEGMA was shown to be more suitable to reduce protein adsorption. The effect of POEGMA architecture on HB-VLP adsorption was also evaluated by using monomers with different branch-chain

length. Adsorbent grafted with a middle branch chain length, $POEGMA_{300}$ showed a 92% flow-through recovery of HB-VLPs, higher than the unmodified adsorbents which recorded 75.9% of flow-through recovery, as well as a 5% improvement over the short chain $POEGMA_{200}$ polymer from a previous study by our research group. The attributes of the polymer modified adsorbents developed shows its potential used to recover HB-VLPs from clarified *E. coli* homogenate.

Publications during Enrolment

1. **H.W. Ng,** M.F.X. Lee, G.K. Chua, B.K. Gan, W.S Tan, C.W. Ooi, S.Y. Tang, E.S. Chan, B.T. Tey, Size-selective purification of hepatitis B virus-like particle in flow-through chromatography: types of ion exchange adsorbent and grafted polymer architecture, *J Sep Sci.* (2018 Feb 9) doi: 10.1002/jssc.201700823.

Collaborations

1. S.L. Lim, **H.W. Ng,** M.A. Akwiditya, C.W. Ooi, E.S. Chan, Kok Lian Ho, W.S. Tan, G.K. Chua, B.T. Tey, Single-step purification of recombinant hepatitis B core antigen Y132A dimer from clarified *Escherichia coli* feedstock using a packed bed anion exchange chromatography. *Process Biochem.* (2018 March 8.) In Press- Corrected Proof. Doi: 10.1016/j.procbio.2018.03.003

Declaration

This thesis contains no material which has been accepted for the award of any other degree or diploma at any university or equivalent institution and that, to the best of my knowledge and belief, this thesis contains no material previously published or written by another person, except where due reference is made in the text of the thesis.

[redacted]

_____

(Ng Hon Wei)

April 2018

Acknowledgement

First and foremost, I wish to express my gratitude to my supervisors, Prof. Beng Ti Tey, Dr Edward Chien Wei Ooi, Dr Patrick Siah Ying Tang and Dr Gek Kee Chua. The support I received throughout was instrumental to the completion of my study. I would also like to thank Prof. Wen Siang Tan and Dr Kok Lian Ho from Universiti Putra Malaysia for providing invaluable advices.

The study was also completed with much needed team support. I appreciate the support and advice from my labmates: Micky Lee, Christine Chiew, Kiang Wei Ho, Hui Peng Lim, Swee Lu Lim, Poay Ling Beh.

Financial support under HDR Scholarship from School of Engineering, Monash University Malaysia is very much appreciated. This study was funded by e-Science grant (06-02-10-SF0255) from the Ministry of Science, Technology and Innovation, Malaysia.

List of Tables

Table		Page
1	Methods of purification for HB-VLPs expressed in *E. coli*	14
2	Modified adsorbents and their respective polymerization conditions. Reaction performed under nitrogen at 60ºC for 3 h with ammonium persulfate as the initiator	43
3	Ionic capacity of adsorbents and the TGA results of modified adsorbents with respect to its unmodified controls	47

List of Figures

Figure		Page
1	Schematic diagram of (a) flow-through chromatography (FC) of *E. coli* homogenate containing HB-VLPs and (b) mechanism of POEGMA chain excluding HB-VLPs from adsorbent surface	3
2	Free radical initiated polymerization of POEGMA on anion exchange adsorbents	22
3	(a) Flow-through protein concentration ratio, C/C_0 with at increasing protein load with respect to the feedstock. SDS-PAGE fractions collected from (b) *E. coli* homogenate containing HB-VLPs and (c) *E. coli* homogenate containing HB-tridimers	28
4	Breakthrough curves for VLPs from *E. coli* homogenate containing HB-VLPs using POEGMA grafted adsorbent	31
5	Protein size distribution of the following: (a) flowthrough fraction of (▬) QFF-C, and (▬ ▪ ▬) QFF-P200 after FC of *E. coli* homogenate containing HB-VLPs, (═) *E. coli* homogenate containing HB-VLPs and (••••••) SEC-purified HB-VLPs while (b) flowthrough fraction of (	33

	▬) QFF-C, and (▬▪▬) QFF-P200 after FC of *E. coli* homogenate containing HB-tridimers and (·····) *E. coli* homogenate containing HB-tridimers	
6	Protein collected in the flow-through fraction of (a) *E. coli* homogenate containing HB-VLPs and (b) *E. coli* homogenate containing HB-tridimers	34
7	Confocal laser scanning microscopy (CLSM) of FITC-labelled HB-tridimer on (a) ungrafted QFF-C, (b) polymer grafted QFF-P200; FITC-labelled HB-VLPs on (c) ungrafted QFF-C, (d) polymer grafted QFF-P200 after batch adsorption	35
8	(a) MrN-VLPs and its HCPs collected in the flow-through fraction and (b) SDS-page results with Lane 1, *E. coli* homogenate containing MrN-VLPs; Lane 2, flow-through pool of QFF-C; Lane 3, flow-through pool of POEGMA grafted Sepharose QFF (QFF-P200)	37
9	FTIR spectra of the following adsorbents: (▬) QFF-C, (– · ·) QFF-P200, (▬▬▬) QFF-P300, (·····) QFF-P500, (▬) QXL-C, (– · –) QXL-P200, (– · –) QHP-C, (▬) QHP-P200.	46
10	(a) Chromatograms of SEC-purified HB-VLP feedstock using adsorbents with different size: QHP-C (35 μm) and QFF-C (90 μm), with QHP-P200 and QFF-P200 representing the respective adsorbent grafted with $POEGMA_{200}$. Absorbance (mAU) for (▬) QHP-C, (– · –) QHP-P200, (▬) QFF-C, and (– · ·) QFF-P200; and (▬) conductivity (mS/cm) against volume of buffer (ml) flowed in the column. (b) Flow-through recovery and PF of HB-VLP from *E. coli* homogenate	49
11	Size distribution in terms of volume based distribution of proteins collected in the a) flow-through fractions, and b) eluted fractions of adsorbents (▬) QHP-C, (▬▪▬) QHP-P200, (▬) QFF-C, and (▬▪▬) QFF-P200, and c) (▬) *E. coli* feedstock and (·····) SEC-purified HB-VLPs.	52
12	Flow-through recovery and PF of HB-VLP from *E. coli* homogenate using standard adsorbents QFF-C, adsorbents grafted with $POEGMA_{200}$	54

(QFF-P200), Sepharose XL adsorbents (QXL-C) and POEGMA grafted QXL-P200

13 Illustration of size-selective exclusion of the HB-VLPs and the larger HCPs from the external surface of adsorbents. The smaller HCPs are able to approach the external surface and pores in the adsorbent. (a) Adsorption of HB-VLPs on the additional binding sites of grafts on the unmodified Sepharose XL adsorbent (QXL-C); the dense $POEGMA_{200}$ grafts on QXL-P200 adsorbent reduced the diffusion of HCPs to external surface of the adsorbent, and (b) Sepharose Q grafted with POEGMA of increasing side chain length increased the exclusion of larger HCPs and HB-VLPs 56

14 (a) Flow-through recovery and PF of FC of HB-VLPs from *E. coli* homogenate and (b) SDS-PAGE results of the feed and flow-through fractions collected. Lanes 1, 2, 3 and 4 represents the fractions purified with QFF-C, QFF-P200, QFF-P300 and QFF-P500 respectively, while (a) represents the first half of flow-through fraction collected and (b) represents the second half of flow-through fraction collected. 57

Abbreviations

APS	Ammonium persulfate
ATR-FTIR	Attenuated total reflectance Fourier transform infrared
BSA	Bovine serum albumin
CLSM	Confocal laser scanning microscopy
CV	Column volume
DEAE	Diethylaminoethyl
DNA	Deoxyribonucleic acid
DTT	DL-Dithiothreitol
E. coli	*Escherichia coli*
FITC	Fluorescein isothiocyanate
HBcAg	Hepatitis B core antigen
HBV	Hepatitis B virus
HB-VLP	Hepatitis B VLP
HCPs	Host cell proteins
IgG	Immunoglobulin
IMAC	Immobilized metal affinity chromatography
IPTG	Isopropyl-β-D-thiogalactopyranoside
LB	Luria Bertani broth
LCST	Lower critical solution temperature
MEO_2MA	2-diethylene glycol methacrylate
M_n	Average molecular weight
$NaHCO_3$	Sodium bicarbonate
Na_2CO_3	Sodium carbonate

OEG	Oligo(ethylene glycol)
OEGMA	oligo(ethylene glycol) methacrylate
$OEGMA_{300}$	Poly[oligo(ethylene glycol) methyl ether methacrylate] M_n = 300g/mol
$OEGMA_{500}$	Poly[oligo(ethylene glycol) methyl ether methacrylate] M_n = 500g/mol
PEG	Polyethylene glycol
PEO	Polyethylene oxide
PF	Purification factor
pI	Isoelectric point
POEGMA	Poly[oligo(ethylene glycol) methacrylate]
SDS-PAGE	Sodium dodecyl sulfate polyacrylamide gel electrophoresis
SEC	Size exclusion chromatography
TEM	Transmission electron microscopy
Tris	Tris(hydroxymethyl)aminomethane
VLP	Virus-like particle

Table of Contents

Copyright Notice ii

Abstract iii

Publications during Enrolment v

Declaration vi

Acknowledgement vii

List of Tables viii

List of Figures viii

Abbreviations xi

Table of Contents xiii

Chapter 1: Introduction 1

1.1. Aims 4

Chapter 2: Literature Review 5

2.1. Virus-like-particles (VLPs) 5

2.2. Purification of VLPs 6

2.3. Flow-through mode ion exchange chromatography 7

2.4. Size exclusion layer on chromatography adsorbents 10

2.5. Inert polymer modification for protein adsorption reduction 12

2.6. Purification of HB-VLP expressed in *E. coli* 13

2.7. Concluding remarks 16

Chapter 3: Size selective flow-through chromatography purification of hepatitis B virus-like particle: effect of protein load and target protein size 17

3.1. Introduction 17

3.2. Materials and Method 19

3.2.1. Chemicals and materials 19

3.2.2. Preparation of clarified *E. coli* homogenate containing HB-VLPs, HB-tridimers or MrN-VLPs 20

3.2.3. Preparation of clarified *E. coli* homogenate containing Noda-virus-like particles 21

3.2.4. Free radical polymerization grafting of POEGMA on anion exchange adsorbents 21

3.2.5. Chromatography of *E. coli* homogenate containing HB-VLPs, HB-tridimers or MrN-VLPs 22

3.2.6. Protein quantitation and protein size distribution 23

3.2.7. Determination of protein size distribution 24

3.2.8. Confocal laser scanning microscopy (CLSM) 24

3.2.9. Calculations 25

3.3. Results and Discussion 27

3.3.1. Breakthrough curves from *E. coli* homogenates containing HB-VLPs and HB-tridimers 27

3.3.2. Optimum protein load for FC using POEGMA grafted adsorbent 30

3.3.3. Chromatography of *E. coli* homogenate containing HB-VLPs or HB-tridimers 32

3.3.4. Effect of protein size on adsorption of HB-VLPs and HB-tridimers under batch condition 34

3.3.5. Applicability of grafted POEGMA on exclusion of MrN-VLPs 36

3.4. Conclusion 38

Chapter 4: Size-selective purification of hepatitis B virus-like particle in flow-through chromatography: types of ion exchange adsorbent and grafted polymer architecture 39

4.1. Introduction 39

4.2. Materials and Methods 41

4.2.1. Chemicals and materials 41

4.2.2. Preparation of clarified *E. coli* homogenate containing HB-VLPs 41

4.2.3. Preparation of HB-VLPs purified with size exclusion chromatography (SEC) 42

4.2.4. Instruments and apparatus 42

4.2.5. Grafting of POEGMA on anion exchange adsorbents 43

4.2.6. Characterization of POEGMA-grafted adsorbent 44

4.2.7. Flow-through chromatography of *E. coli* homogenate and chromatography of SEC-purified HB-VLPs 45

4.2.8. Quantification of protein 45

4.3. Results and Discussion 46

4.3.1. Characterization of adsorbents 46

4.3.2. Effect of adsorbent size on HB-VLPs adsorption 47

4.3.3. Comparison between charged dextran grafts and POEGMA grafts for FC 53

4.3.4. Effect of the branch chain length of grafted POEGMA 55

4.4. Conclusion 58

Chapter 5: General Discussion, Conclusion and Recommendation for the Future Work 60

5.1. General discussion 60

5.2. Conclusion 61

5.3. Recommendations for future work 61

References 63

Chapter 1: Introduction

Virus-like particles (VLPs) are non-infectious viral structural protein that resembles viruses. These highly antigenic VLPs hold promising application in vaccine development, targeted drug and gene delivery [1]. With recent improvements in upstream processes that increase yields and harvest volumes, downstream processing (DSP) is becoming increasingly important in shaping higher overall productivity and lower cost [2].

The separation of VLPs from its HCPs can be performed based on differences in size, charge, or a combination of both [3]. Size exclusion chromatography (SEC) is a direct way of purifying HB-VLPs, but its low productivity and scalability due to long run-time, low recovery, product dilution and low capacity makes it undesirable for large scale process. Thus, SEC is primarily used as an analytical tool while separations based on electrostatic interactions by ion exchange chromatography (IEC) are usually preferred for preparative separation [4].

Generally, the size of VLPs ranges from 22 to 200 nm in diameter, as they are self-assembled from multiple subunits or monomer [5]. However, the pore size of an agarose-based adsorbent is approximately 50 nm [6]. The large size of VLPs assembled from hepatitis B core antigen (HBcAg) has been shown to reduce the intraparticle diffusion in porous ion exchange adsorbent during bind-and-elute chromatography, which in turn affects its adsorption and recovery [7]. Negative impacts in terms of slower adsorption kinetics [8] and disassembly (i.e. disintegration) of multi-subunits structure of the VLP [5] have been well documented. Thus, flow-through chromatography (FC) where contaminants are adsorbed while VLPs are collected in flow-through is a viable alternative to bind-and-elute mode chromatography [2]. Since VLPs can still be adsorbed on adsorbent's external surface [9], polymer modified FC adsorbent has been used to reduce the HB-VLPs adsorption in order to improve the separation HB-VLPs from its HCPs.

FC is more commonly used for polishing step whereby purified protein samples are polished by removing low amount of impurities that are closely related to the target protein [10,11]. In contrast, the application of FC in primary isolation step involving the separation of the target protein from large quantity of HCPs. Thus the process requires adsorbent with the capacity to remove large amount of impurities. In other words, the low throughput of FC will be the main hurdle limiting its application as primary isolation step at preparative scale.

Furthermore, most reported studies of FC were aimed at the exclusion of viruses with hydrodynamic diameter (D_H) in the 70-100 nm range [12], which are larger than the pores of standard adsorbents [approximately (50-70 nm)]. Hence, the separation of smaller HB-VLP (~32 to 36 nm) from its HCPs [13] will be more challenging to the conventional diffusive adsorbent. As HB-VLPs are smaller than the average pore size of adsorbents, POEGMA-grafts were needed to selectively exclude HB-VLPs and to reduce the undesirable adsorption of HB-VLPs on the surface of the adsorbents.

In previous study, FC purification of HB-VLPs from *E. coli* homogenate with a standard size Sepharose Q FF adsorbent grafted with inert polymer poly(ethylene glycol) methacrylate (POEGMA) was successfully implemented. A satisfactory HB-VLPs recovery (>80%) and 2 mg HCPs removed/ml of adsorbent have been achieved [14]. Even though the adsorbents were successfully employed in primary isolation step chromatography, the FC performance and the adsorption of HB-VLPs of the adsorbent was not evaluated at different protein load.

Therefore, the main objective of this study was to develop a FC adsorbent with size selective adsorption properties for the purification of HB-VLP from *E. coli* homogenate. As depicted in Figure 1, the grafted POEGMA on the adsorbents reduces the mass diffusion and adsorption of the HB-VLPs while maintaining the adsorption of the smaller size HCPs.

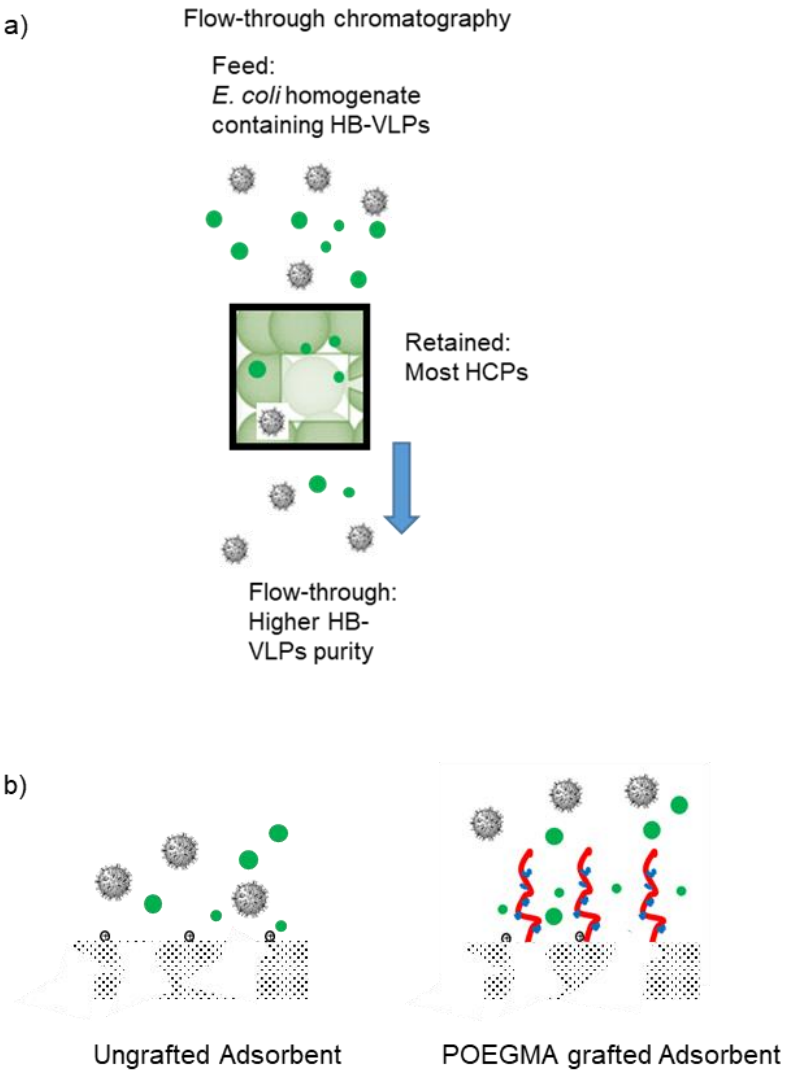

Figure 1. Schematic diagram of (a) flow-through chromatography (FC) of *E. coli* homogenate containing HB-VLPs and (b) mechanism of POEGMA chain excluding HB-VLPs from adsorbent surface

1.1. Aims

The present study aims to establish POEGMA modified adsorbent as an initial isolation FC purification process. The investigation was divided into two phases.

1. The 1st phase - Chapter 3 aims to evaluate the effect of feedstock condition such as target protein size and protein load on the FC performance. The specific objectives of this phase are:
    a. To assess the effect of the target protein (HBcAg) size on the adsorption capacity of adsorbent
    b. To determine the optimum protein load of *E. coli* homogenate with HB-VLPs using POEGMA grafted adsorbent,
    c. To assess the applicability of POEGMA grafted adsorbents to recover other VLPs from clarified *E. coli* homogenate.

Once the optimal protein load for FC of HB-VLPs are obtained, the design of the grafted adsorbents are further studied to improve the FC performance

2. The 2nd phase – Chapter 4 aims to further evaluate the effect of the design of polymer grafted FC adsorbent on the FC performance. The specific objectives of this phase are:
    a. To determine the effect of the adsorbent's accessible surface area on FC performance
    b. To determine the effect of functionality of polymer grafts on FC performance
    c. To evaluate the effect of POEGMA's ethylene oxide branch chain length on FC performance

Chapter 2: Literature Review

2.1. Virus-like-particles (VLPs)

VLPs are empty structural protein of viruses that do not contain any genetic materials. Therefore, they are non-replicating and non-infectious. To date, over 110 VLPs from more than 35 virus families have been constructed [15]. Some were developed for fundamental research purposes while most are aimed to be used in vaccines development [16]. VLPs are relatively safer to use compared to the live or attenuated virus particles as a vital platform for vaccines development [17]. To date, notable vaccines based on VLP include hepatitis B virus (HBV) and human papillomavirus (HPV). VLPs have also been widely applied in multivalent vaccine development to induce humoral and cellular immune responses, and utilized in diagnosis test to detect a wide range of infectious diseases, among other applications [18].

One such VLP is hepatitis B core antigen VLP (HB-VLP), an icosahedral nucleocapsid assembled from monomers of hepatitis B core antigen (HBcAg). The nucleocapsid structure consists of 180 or 240 subunits with triangulation number $T = 3$ or $T = 4$ [1]. The proper assembly of HB-VLP is vital for its immunogenicity [19]. The distinctive structure of HB-VLP can stimulate the body's immune system to secrete antibodies [20], thus HB-VLP has been successfully employed as a vaccine carrier [21] and as an active component of hepatitis B vaccine [22].

2.2. Purification of VLPs

Advances in upstream processing in recent years have increased recombinant protein yields, making downstream processing increasingly pivotal in determining overall productivity and cost of recombinant protein production [2]. Protein purification process aims to separate the target protein from the impurities. The impurities include process-related impurities such as reagents and additives (antibiotics and nucleases), or cell substrate impurities such as HCPs, nucleic acids, and proteoglycans. Whereas product-related impurities include aggregates of virus and free envelope proteins [23].

The separation of VLP from its HCPs can be based on differences in size, charge, hydrophobicity and affinity [3]. Over the years, the expression level of HB-VLP has increased from 7% [24] to 30% of total proteins in *E. coli* homogenate [25]. The increased load of proteins in the feedstock necessitates improved unit operation for higher recovery. Although size exclusion chromatography (SEC) have been used to separate VLPs from its cell homogenate with high purity of > 90% [26], these processes have poor scalability due to low flow rates and low capacity. On the other hand, separations based on electrostatic interactions by ion exchange chromatography (IEC) are usually preferred for preparative and large scale applications [23].

In general, ion exchange chromatography is a widely applied technique for separation and purification of large proteins such as VLPs. However, the structure of VLPs is vulnerable to disintegration during binding and eluting steps, a problem that is especially prevalent with standard diffusive agarose-based adsorbents. Additionally, the small pore size (approximately 50-70 nm) found in these adsorbent has resulted a slow intraparticle diffusional transport of the VLPs [27], which in turn causes a significant reduction in VLPs adsorption [7].

The challenges with mass diffusion of large proteins in diffusive adsorbents can be addressed with a new generation of adsorbents. These perfusion adsorbents possess large micron range pores designed to provide better mass transport to large proteins. This in turn improves the adsorption of these large proteins [5,8,28]. However, large pores that are more than 6 µm or 10 times the hydrodynamic radius (D_H) were required to obtain satisfactory recovery for large virus particles [29]. Besides, the stability and correct assembly of VLP recovered using bind-and-elute mode is another concern [30]. A study by Yu et. al. [11] using perfusion adsorbent DEAE AP 280nm (approx. 10 times larger than the VLP's D_H), reported a 25% disintegration of the recovered VLPs [5]. These modified adsorbents are also designed with increased surface area in order to improve accessible of ligands, leading to inherent drawbacks such as increased impurity binding to the adsorbents [31]. Reducing the ligand density on ion exchange adsorbents have been shown to be effective in maintaining the structure of VLP during bind-and-elute process. However, such strategy would necessitate longer column and in turn causes difficulty in scaling up the process [32].

2.3. Flow-through mode ion exchange chromatography

The difficulty in recovering VLPs with standard diffusive adsorbents makes flow-through chromatography (FC) a viable alternative to bind-and-elute mode. In FC, the impurities are adsorbed while the target protein pass through the column and is recovered in the flow-through fraction. Generally, FC shortens the processing time, and circumvents other post-processing (i.e. desalting) of the product [33,34], especially when it is dealing with high protein load feedstock [35]. In addition, the bioactivity of the product purified with FC is well preserved with minimal product loss since the VLPs does not have strong interaction with the adsorbent.

Different modes of interaction including ion exchange [11], hydrophobic interaction [33], and specific interaction such as immune-affinity [36] are used in FC. However, it is challenging to operate FC using selective ligands such as immune-affinity is dealing with heterogeneous and complicated mixture of impurities [37–39]. Thus, thorough screenings for suitable ligand are often necessary.

In this study, ion exchange chromatography was used, as this mode of purification is still the workhorse of the industry. FC has been commonly applied to remove trace impurities from monoclonal antibody IgG feed streams [40–43]. Viruses [31], enzymes [44], Hb (haemoglobin) [45] and cell surface proteins [40] have also been polished using FC to remove the impurities.

Purification of IgG using FC has shown to be efficient in human serum albumin (HSA) removal that has been resulted in an increase in IgG purity from 20% to 90% with a purification factor 4 - 4.5 [46]. As isoelectric point of HSA is generally in acidic range of pI=4.4 while IgGs commonly have pI=5.5-8, resulting in a stark difference of adsorptive behaviour between the two species. This has allowed a high flow-through recovery and PF of the IgG using FC.

However, the HB-VLPs and its HCPs possess similar adsorptive behaviour due to overlapping isoelectric point [47,48], likely causing unwanted adsorption of the target protein As such, difference of size between target protein and impurities can be used to improve the separation. Currently, some reported studies of FC were aimed at the exclusion of large viruses, such as adenovirus (70-100 nm) [12] and influenza virus (80-120 nm) from smaller size HCPs [31]. However, our research group focuses on the purification of smaller HB-VLP (~32 to 36 nm) that are more challenging to separate from its HCPs [13]. Thus, an additional size exclusion layer is required to reduce the adsorption of the target HB-VLPs to improve flow-through recovery.

2.4. Size exclusion layer on chromatography adsorbents

One straightforward method to reduce undesired adsorption of target VLPs in FC can be achieved by using larger adsorbent. Larger adsorbent possesses lower external surface area to volume ratio (eSA:V) that in turn reduce the target virus's interaction with ligand [31]. However, the adsorption capacity of HCPs for large adsorbent is low, hence, a poor resolution or purification factor of VLP is expected.

Alternatively, size selective inert layer can be employed in FC adsorbent design. Size selective FC adsorbents coated with inert layer were developed primarily for analytical scale separations, method otherwise known as restricted access media (RAM) analysis. Protein-coated porous silica was used to remove small molecules for drug analysis in plasma [49]; setting the foundation for new methods to separate smaller proteins [50–52]. RAM concept was also employed in developing adsorbents made from silica supports with an hydrophilic polymer (silicone) coating acting as a semi-permeable layer [53]. Similarly, RAM with strong cationic group was employed to identify heroin metabolites in human urine [54]. Adsorbents with well-defined molecular weight cut-off have been used, one example is the mesoporous silica adsorbent with narrow pore size distribution. The adsorbent successfully produced sharp extractions of peptides from human plasma [55] and separation of serum phosphopeptides [56].

Since common adsorbents do not possess narrow pore size distribution, modification with a semi-permeable inert layer on adsorbent can be effective in reducing unwanted adsorption of large proteins. Ion exchange adsorbents such as Sepharose DEAE FF or Streamline DEAE have been modified with inert agarose outer shell to exclude large nano-particles of bovine serum albumin, resulting in up to 10-fold increase in flow-through recovery [57,58]. Ion exchange adsorbent had also been modified with hydroalkyl-group based neutral coating to exclude plasmid molecules [59].

The inert layer coated on the surface adsorbent can be modified to different molecular weight cut-off point. For instance, CaptoCore^{TM} 700 has a molecular weight cut-off point of 700 kDa compared to Q Sepharose HP that has a molecular weight cut-off point of 4000 kDa. [60,61]. CaptoCore^{TM} 700 has been used to remove trace impurities from adenovirus in the polishing step [62] and to remove HCPs and DNA from influenza A and B viruses in FC [10]. However, a core shell adsorbent similar to CaptoCore^{TM} 700, Inert layer 1000, was reported to result in significant entrapment and product loss when challenged with *E. coli* homogenate containing HB-VLPs [63]. Diffusional resistance by the inert layer of core shell model has also been reported to limit the access of proteins (impurities) to the internal binding surface of the adsorbents, and hence reduce the adsorption rate of impurities [31]. The lower adsorption rate of impurities has resulted a long adsorption time or long column length that limits its applicability on large and preparative scale.

2.5. Inert polymer modification for protein adsorption reduction

Modification of ion exchange adsorbents with inert polymer can reduce adsorption of HB-VLPs and in turn improve its flow-through recovery [63,64]. The concept of grafting ethylene oxide based polymer to reduce adsorption of protein is based on poly(ethylene oxide) (PEO) polymer layer well known ability to suppress protein adsorption on modified/grafted surface [68]. The hydrophilicity of polymer and the steric hindrance of polymer layer exerted on the approaching protein are believe to be the mechanism that suppress the protein adsorption [65]. Beside PEO, there are a number of other promising antifouling polymers, namely zwitterionic polymers, poly(hydroxyl functional acrylates), poly(2-oxazoline)s, poly(vinylpyrrolidone), and poly(glycerol) [66]. However, PEO is still the most widely used polymer for reducing protein adsorption and it is inert to most charged proteins [66]. The ability of the grafted PEO layer to reduce protein adsorption is based on the steric repulsion that decreases the direct contact between proteins and the underlying surface and the hydration shells which limits the secondary adsorption of proteins onto the polymer itself [67]. Another proposed mechanism involves electrostatic charging effect due to the well-ordered monolayers of oligo(ethylene glycol) [68].

Key characteristic of grafted polymer such as grafting density, chain length and architecture, depend on the polymerisation technique. The key factor affecting protein resistance is grafting density; even with short chain length, grafted PEO could still resist the adsorption of protein provided that the surface has a sufficient polymer coverage [69]. Densely grafted POEGMA brushes have been shown to produce excellent anti-fouling surfaces that resist protein adsorptions [70]. The effect of hydrophilicity of the polymer was found to be less significant compared to the surface density of polymer [71]. Thus, densely grafted polymer can negatively impact the impurities clearance of the adsorbent, as polymer density should be sufficiently low for HCPs to penetrate while excluding target protein (i.e. the large HB-VLPs). Since low grafting density have been shown to sufficiently exclude much smaller bovine serum albumin (BSA) [72], conventional free polymer radicalisation was used by our research group to graft POEGMA on ion exchange adsorbents [64] as the method has been shown to improve the size-selective properties of polystyrene latex beads used for size exclusion chromatography [73].

Finally, the resistance to protein adsorption by the grafted polymer is also dependent on its architecture [74]. For example, the POEGMA with ethylene oxide branch chain have been shown to be more effective than linear chain PEG [70]. Hence, the effect of polymer architecture in size selective exclusion of HB-VLPs requires further study.

2.6. Purification of HB-VLP expressed in *E. coli*

Small scale [75] and large scale production of recombinant HB-VLP from *E. coli* have been successfully carried out, with expression level of HB-VLP at 30% of total proteins in *E. coli* [25]. Purification of HB-VLPs has been performed with different purification techniques as shown in Table 1.

Table 1. Methods of purification for HB-VLPs expressed in *E. coli*

Method of purification	Recovery (%)	Purity (%)	Purification steps (Time required)	References
Sucrose gradient ultracentrifugation[*a]	30	93	>3 steps (48-72 h)	[76]
Size exclusion chromatography[*a]	30	85	2 steps (12-15 h)	[13,24]
Native agarose gel electrophoresis and electroelution [*a]	40	90	2 steps (4 h)	[13]
Immobilized metal affinity-expanded bed adsorption chromatography [*b*c]	56	91	2 steps (2 h)	[77]
Ion exchange expanded bed adsorption chromatography (bind-and-elute mode) [*a*c]	50.7	50	2 steps (2 h)	[4,78]
M13 Phage immobilised expanding bed adsorption chromatography [*a*c]	45	44	2 steps (6 h)	[78]
Ion exchange FC[*a*c]	60	65	3 steps (2 h)	[14]

[*a] Additional clarification step required (pre-processing of feedstock)

[*b] Additional removal of His-tagged required

[*c] Further polishing step required

As shown in Table 1, expanded bed adsorption chromatography offers satisfactory recovery, short processing time and the capacity to process large amount of feedstock [4,77–79]. However, biomass interactions and aggregations onto adsorbent are limitations commonly associated with expanded bed chromatography [80]. Additionally, several key challenges of ion exchange expanded bed adsorption chromatography include limited recovery due to steric hindrance exerted by the adsorbed cell debris and HB-VLP [77] as well as low intraparticle mass diffusion of HB-VLPs in standard porous adsorbent [79].

Immobilized metal affinity chromatography (IMAC) utilises a specific metal affinity to adsorb HB-VLPs, which improves its product purity significantly compared to ion exchange (Table 1) [77]. However, IMAC requires the target protein to possess a special histidine peptide tag and it necessitates a post processing step to remove the histidine tag. On the other hand, purification based on size differences such as size exclusion chromatography can provide high product purity [24,76]. However, the process is tedious (12-14 hour of run-time), the recovery is low (20%), and the processing capacity is much lower (0.4 mg of total protein/ ml adsorbents) compared to ion exchange chromatography (IEC) (1-2 hour run-time, 80-90% recovery and processing capacity of 10 mg total protein/ml adsorbent).

Among the available methods to purify HB-VLPs, ion exchange chromatography is non-specific. Thus, the effects of polymer grafts can be applicable for separation of other types of viruses and VLPs from their smaller HCPs. Besides, packed bed chromatography is widely used and are readily scalable.

HB-VLP and its HCPs possess similar adsorptive behaviour – more than 90% of HCPs are acidic (isoelectric point range = 4.53 – 6.72) [47], which overlaps with the pI of HB-VLP (pI= 4.0) [48]. Hence, there is a need to use a size selective polymer layer to improve separation of HB-VLPs from its HCPs [17]. Study of POEGMA grafted adsorbent on expanded bed chromatography was avoided to reduce unwanted interaction from cell debris.

In short, FC enables better preservation of the VLP structure with minimal effect on the antigenicity. Furthermore, the impurities removal capacity is sufficiently high at 2 mg of impurities removed/ ml adsorbent [63]. Thus, the focus of this study is to improve the performance of FC for the purification of HB-VLPs.

2.7. Concluding remarks

The literature survey presented reveals several research gaps as well as limitations in the current adsorbent design for FC. One related area that can also be explored is the primary isolation step for VLPs, especially the selectivity and performance at different protein load. Investigation would outline the applicability and scalability of diffusive porous adsorbent. As for the polymer itself, a previous study has demonstrated the effect of longer POEGMA chain length on the FC performance [64]. However, the architecture of the POEGMA i.e. the ethylene oxide branch chain was not explored. Hence, the objective of the project was the development of FC adsorbent for the purification of HB-VLP from *E. coli* clarified lysate, in terms of purification factor (PF) or recovery of HB-VLP.

Chapter 3: Size selective flow-through chromatography purification of hepatitis B virus-like particle: effect of protein load and target protein size

3.1. Introduction

Hepatitis B core antigen (HBcAg) virus-like particles or HB-VLPs are the potential delivery vehicles for gene and drug [81], as well as the universal carriers of multi-component vaccines [77]. The large size of HB-VLPs have been reported to significantly reduce its intraparticle diffusive mass transport in porous ion exchange adsorbents (diffusive adsorbents), which in turn affects its adsorption [7]. Thus, flow-through chromatography (FC) i.e., contaminants adsorbing to the adsorbent and VLPs particles collected in flow-through is a viable alternative to bind-and-elute mode chromatography [2].

However, FC are usually used for polishing step in which the amount of impurities adsorbed are usually low. For example, conventional diffusive anion exchange adsorbent was used to adsorb DNA - up to 0.2 mg DNA/ml adsorbent [10], while another study showed adsorption of 0.005 mg Chinese hamster ovary HCPs/ml of adsorbent [11]. However, to establish FC as a primary isolation step, the HCPs binding capacity at protein load higher than the conventional polishing step should be determined.

Since clarified homogenate containing VLPs that have low intraparticle mass transport in standard diffusive adsorbents, the effect of the target protein (HBcAg) size on the HCPs clearance should be investigated. Two different *E. coli* feedstocks were employed, one containing HBcAg virus-like-particles (HB-VLPs) which consist of 183 – 240 units of HBcAg monomers. The other feedstock contains a much smaller variant of HBcAg called HBcAg-Y132A, that consist of a total of 6 units of HBcAg monomer, in the form of 3 units of dimer or 'trimer of dimers structure' (referred to as HB-tridimer) [82]. Comparison between the two feedstocks should elucidate the effect of target protein size on the adsorption capacity of the adsorbent.

Besides, partial displacement of proteins by more favourably adsorbed ones due to competitive binding have been reported [83]. Partial displacement has also been observed by loading protein beyond anticipated breakthrough [84]. Thus, the effects of the protein load on the selectivity and performance of FC should also be investigated.

In this chapter, analysis of breakthrough curve with *E. coli* homogenate containing HB-VLPs was performed to determine the optimum range of protein loading for better chromatography performance. Besides, reduction of HB-VLPs adsorption due to POEGMA grafted adsorbents under different protein load was evaluated. FC operation with *E. coli* homogenate containing HB-tridimers was performed to evaluate the effect of the target protein size on the adsorption of HBcAg and HCP. Chromatography of Noda virus-like particles (MrN-VLPs) was also performed to demonstrate the applicability of POEGMA's size selective exclusion on other VLPs.

3.2. Materials and Method

3.2.1. Chemicals and materials

Anion exchange agarose adsorbents, namely Sepharose Q FF was purchased from GE Healthcare (Switzerland). Monomers for grafting of POEGMA including di(ethylene glycol) methyl ether methacrylate (MEO_2MA), polyethylene glycol methacrylates of M_n=300 ($OEGMA_{300}$) were sourced from Sigma-Aldrich (Singapore). Prior to the polymerization reaction, the monomers were purified with a neutral alumina flash chromatography. Ammonium persulfate (APS) was sourced from Acros Organics (Geel, Belgium). Ready-to-use Bradford assay dye reagent was purchased from Nacalai Tesque (Japan). SEC-purified HB-VLPs (90% purity) and HB-tridimers (90% purity) was provided by Department of Pathology, Faculty of Medicine and Health Sciences, Universiti Putra Malaysia. Both pure protein samples were stained with FITC Isomer I (Sigma-Aldrich, Singapore). Anhydrous dimethyl sulfoxide (DMSO), sodium carbonate (Na_2CO_3), sodium bicarbonate ($NaCO_3$) and ammonium chloride (NH_4Cl) were also sourced from Sigma-Aldrich, Singapore.

3.2.2. Preparation of clarified *E. coli* homogenate containing HB-VLPs, HB-tridimers or MrN-VLPs

The preparation of clarified *E. coli* homogenate containing HB-VLPs was performed according to protocol described in Ng et al. [25]. The cells of *E. coli* strain W311OIQ expressing HB-VLPs, were cultured in Luria Bertani (LB) medium containing 100 µg/mL ampicillin at 37 ºC with a shaking speed of 250 rpm. When the absorbance at 600 nm reached 0.8 – 1.0, expression of HB-VLPs was induced by adding isopropyl β-D-1-thiogalactopyranoside (IPTG) to a final concentration of 1 mM. The protein expression was continued for another 16 h at 37 ºC. Centrifugation at 3,836 *g* (Heraeus™ Multifuge™ X1 Centrifuge, Thermo Scientific, USA) for 20 min at 4 ºC were used to harvest *E. coli* cells from the culture broth. The harvested cell pellet was resuspended at 10% w/v in 25 mM of Tris-HCl buffer, pH 8.0. The cell suspension was disrupted with ultrasonication (Q500 Sonicator, Q Sonica, United States) at 40% amplitude (20 min with 30 s intervals in between pulses). The clarified homogenate was obtained by centrifugation at 12,000 g at 4 ºC for 20 min, and used as initial feedstock for subsequent chromatography.

Similar to HB-VLPs, the cells of *E. coli* strain W311OIQ with the pR1-11E plasmid, expressing the truncated HBcAg-Y132A (i.e. HB-tridimers) were cultured and subsequently harvested. The harvested cell pellet was resuspended in 25 mM of Tris-HCl buffer, pH 8.0, 0.1 mM DL-Dithiothreitol (DTT) to avoid agglomeration of the tridimer structure. The cell disruption and the subsequent cell lysate calcification including ultrasonication and centrifugation was performed as described in the paragraph above.

3.2.3. Preparation of clarified *E. coli* homogenate containing Noda-virus-like particles

Transformant with the recombinant plasmid harboring the sequence of the Noda-virus-like particles (MrN-VLP) protein was cultured in 50 ml of LB broth containing ampicillin (100 µg/ml). Incubated at 37°C and shaking speed of 220 rpm was performed overnight. The culture was then transferred into LB broth (at 2 % inoculum size) and further incubated at 37°C at 220 rpm for 2 h until an absorbance at 600 nm of 0.6 to 0.8 was reached. IPTG was then added to the culture (to a concentration of 1 mM) for induction. Another 4 h of incubation of the culture was conducted at 25°C and 220 rpm before harvest. The *E. coli* cells were then pelleted by centrifugation at 3,750 g for 5 min. Then, 10% (w/v) of cell pellet was resuspended in 25 mM of Tris-HCl buffer, pH 8.0. The cell disruption and the subsequent cell lysate calcification was performed as been described in Section 3.2.2.

3.2.4. Free radical polymerization grafting of POEGMA on anion exchange adsorbents

The grafting of POEGMA polymer onto Q Sepharose FF was performed according to the steps outlined by Lee et al. [85]. An example of the reaction formula of graft polymerization and the molecular architecture of POEGMA polymer on QFF-C is depicted in Figure 2. Briefly, 20 ml of 50% (v/v) ethanol solution containing 10% (w/v) or 2 g of filtered adsorbents Sepharose Q FF (QFF-C) was purged with nitrogen for 30 min. Next, 2 ml of pre-purged APS solution (1 M) i.e. 1 mmol APS/g adsorbent was used. Then, the mixture was equilibrated at 60 °C for 15 min. Under an airtight condition, pre-purged monomer solution (MEO_2MA and $OEGMA_{300}$ at 10:1 mole ratio, total of 2 mmol) was transferred to the mixture. The mixture was reacted at 60°C for 3 h. After the reaction, the adsorbents were filtered and washed with a gradually reduced concentration of ethanol solution (80%, 60%, 40%, and 20%

ethanol). Lastly, the adsorbents were washed with a copious amount of deionized water. The grafted adsorbent is abbreviated as QFF-P200, while the grafted polymer as $POEGMA_{200}$.

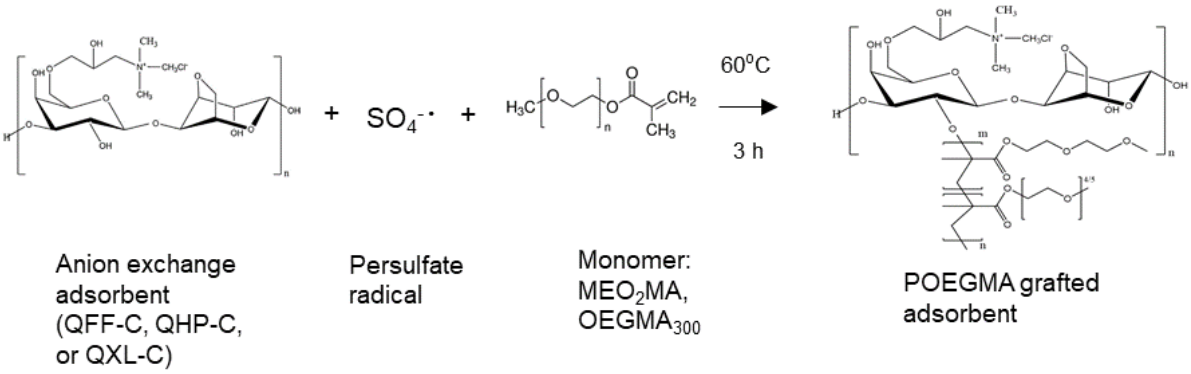

Figure 2. Free radical initiated polymerization of POEGMA on anion exchange adsorbents

3.2.5. Chromatography of *E. coli* homogenate containing HB-VLPs, HB-tridimers or MrN-VLPs

Chromatography of the clarified *E. coli* homogenate was done with an AKTA Purifier 10 (GE Healthcare, USA). The chromatogram was recorded at wavelength of 280 nm. The 1.0 ml columns were purchased from BioToolomics (United Kingdom).

For breakthrough curve analysis, the feedstock was continuously loaded with Superloop 10 ml (GE Healthcare, USA), 0.25 ml fractions are collected using the fraction collector Frac–900 (GE Healthcare, USA) as the loading proceeded. Regeneration of the adsorbents were subsequently performed by flowing 20 ml of Buffer B (11 ml; 25 mM Tris–HCl; pH 8.0; 1 M NaCl) through the column.

While for FC, 5 ml of Buffer A (25 mM Tris–HCl; pH 8.0) was first loaded to the column for equilibration. Subsequently, 0.5 ml of HB-VLP feedstock (i.e., *E. coli* homogenate, containing 5.8 mg of total proteins and 35.5 – 37.0% of HB-VLPs) was loaded to the chromatography column. Then, 2.5 ml of Buffer A was flowed through the column followed by 0.2 ml of Buffer A to wash off the unbound proteins. Subsequently, an isocratic elution was performed using Buffer B. The chromatography of *E. coli* homogenate containing HB-tridimers was performed in the same way, 0.5 ml of *E. coli* homogenate with HB-tridimers (containing 5.9 mg of total proteins and 37.0% of HB-tridimer) was performed with the same protocol.

For MrN-VLP purification, 0.5 ml of the feedstock (2.1 mg total protein, 7.7% MrN-VLP) was performed with a similar protocol, on a 0.33 ml chromatography column. 2.5 ml of Buffer A was flowed through the column after injection followed by 0.2 ml for washing. Subsequently, an isocratic elution was performed using 6 ml of Buffer B.

3.2.6. Protein quantitation and protein size distribution

The protein concentration (with respect to mg BSA/ml) was quantified using the Bradford assay [86]. Briefly, 10 µL of sample solution was added into a microtiter plate well, followed by 200 µL of ready-to-use Bradford reagent (Bio-Rad). The plate is incubated at room temperature for 5 mins before measuring the absorbance at 595 nm with Sunrise^{TM} microplate reader (Tecan Ltd., Switzerland).

The purity of HB-VLPs was evaluated using sodium dodecyl sulfate-polyacrylamide gel electrophoresis (SDS-PAGE). Firstly, 2x Laemmli Sample Buffer were added to the sample at 1:1 ratio, with DTT added to a final concentration of 50 mM. Subsequently, the mixture was heated at 95°C for 5 min [87]. The resolving gel of 15% w/v acrylamide was electrophoresed for 60 min at 120 V using Mini-PROTEAN® Tetra cell (Biorad, USA). The gel was then stained with staining solution containing 2.5 % wt Coomassie Brilliant Blue R-250, and subsequently destained with a solution containing 10% (v/v) acetic acid and 10% (v/v) methanol. Gel Doc™ XR+ System (Bio-rad, USA) was used to obtain the images of stained gels from SDS-PAGE using Image Lab™ software. The purity of HB-VLPs was obtained from the densitometric analysis of gels. The ratio of the intensity of the HBcAg band (17kDa) to that of all the protein bands was used as to determine the purity of HB-VLPs, as described in Tey et al. [75].

3.2.7. Determination of protein size distribution

A particle size analyzer (Malvern, model Zetasizer Nano ZS, UK) equipped with He-Ne laser (633 nm) was used to determine the size distribution of protein samples, with 2 min equilibration at 25ºC in the automatic optimization mode. The total protein concentration of both feedstocks were adjusted to 1.0 to 1.5 mg/ml, prior to analysis with dynamic light scattering.

3.2.8. Confocal laser scanning microscopy (CLSM)

Confocal laser scanning microscopy (CLSM) was used to evaluate the distribution of adsorbed HB-VLPs or HB-tridimers within the adsorbent. Pure samples of HB-VLPs and HB-

tridimers were fluorescently labelled with FITC Isomer I (Sigma-Aldrich, Singapore) overnight at 4 ºC separately [88]. Excess fluorescent molecules were removed from FITC-labelled HB-VLPs and HB-tridimers via dialysis for 5 cycles (2 h each) with Buffer A, then the concentration of FITC-HB-VLPs and FITC-HB-tridimer were adjusted to 1 mg/mL using Buffer A. For the batch adsorption, 0.1 g of the adsorbent (QFF-C or QFF-P200) was separately introduced to 5 ml of the above FITC stained protein, and the mixture was incubated for 6 h. After the adsorption, the adsorbents were washed by Buffer A for four times. CLSM observation was performed using Nikon Confocal C1 (Nikon, Japan). The laser provided excitation at 488 nm, with the emitted fluorescent light detected between 500 and 545 nm. Images were a single confocal scan averaged three times, collected with 1024/1024 resolution and processed with NIS-Elements C (Nikon, Japan).

3.2.9. Calculations

Purity and recovery of target protein were determined using Eq. 3-1 and Eq. 3-2, respectively:

$$\text{Purity} = \frac{\text{Amount of target protein}}{\text{Amount of total protein}} \times 100\% \qquad \text{(Eq. 3-1)}$$

$$\text{Flow} - \text{through recovery (\%)} = \frac{\text{Amount of target protein in flow-through fraction}}{\text{Amount of target protein in feedstock}} \times 100\% \qquad \text{(Eq. 3-2)}$$

Purification factor (PF) is the ratio of target protein purity in flow-through fraction to the target protein purity in feedstock:

$$\text{PF} = \frac{\text{Purity of target protein in flow-through fraction}}{\text{Purity of target protein in feedstock}} \qquad \text{(Eq. 3-3)}$$

The total protein loss was defined as the protein not collected in the elution and flow-through fraction, and was calculated as below:

$$\text{Total protein loss (\%)} = \frac{\text{Amount of total protein in (feed}-\text{(flow}-\text{through+elution))}}{\text{Amount of Total protein in feed}} \times 100\% \quad \text{(Eq. 3- 4)}$$

3.3. Results and Discussion

3.3.1. Breakthrough curves from *E. coli* homogenates containing HB-VLPs and HB-tridimers

Analysis of breakthrough curve provides an insight into the interaction between the target proteins (i.e. HB-VLPs or HB-tridimers) with the adsorbent in comparison to their respective HCPs. From Figure 3(a), it is apparent that HCPs from *E. coli* homogenate containing HB-VLPs are preferentially adsorbed, as the concentration ratio in the flow-through, C/C_0 value of HB-VLPs is consistently higher compared to its HCPs. In contrast, the HB-tridimers were adsorbed preferentially compared to its HCPs. This is an expected trend as the low intraparticle diffusion of HB-VLPs within the adsorbent causes a markedly lower adsorption. On the other hand, the smaller HB-tridimers has higher intraparticle diffusion, hence is able to compete with HCPs for adsorption in the inner sites of adsorbent.

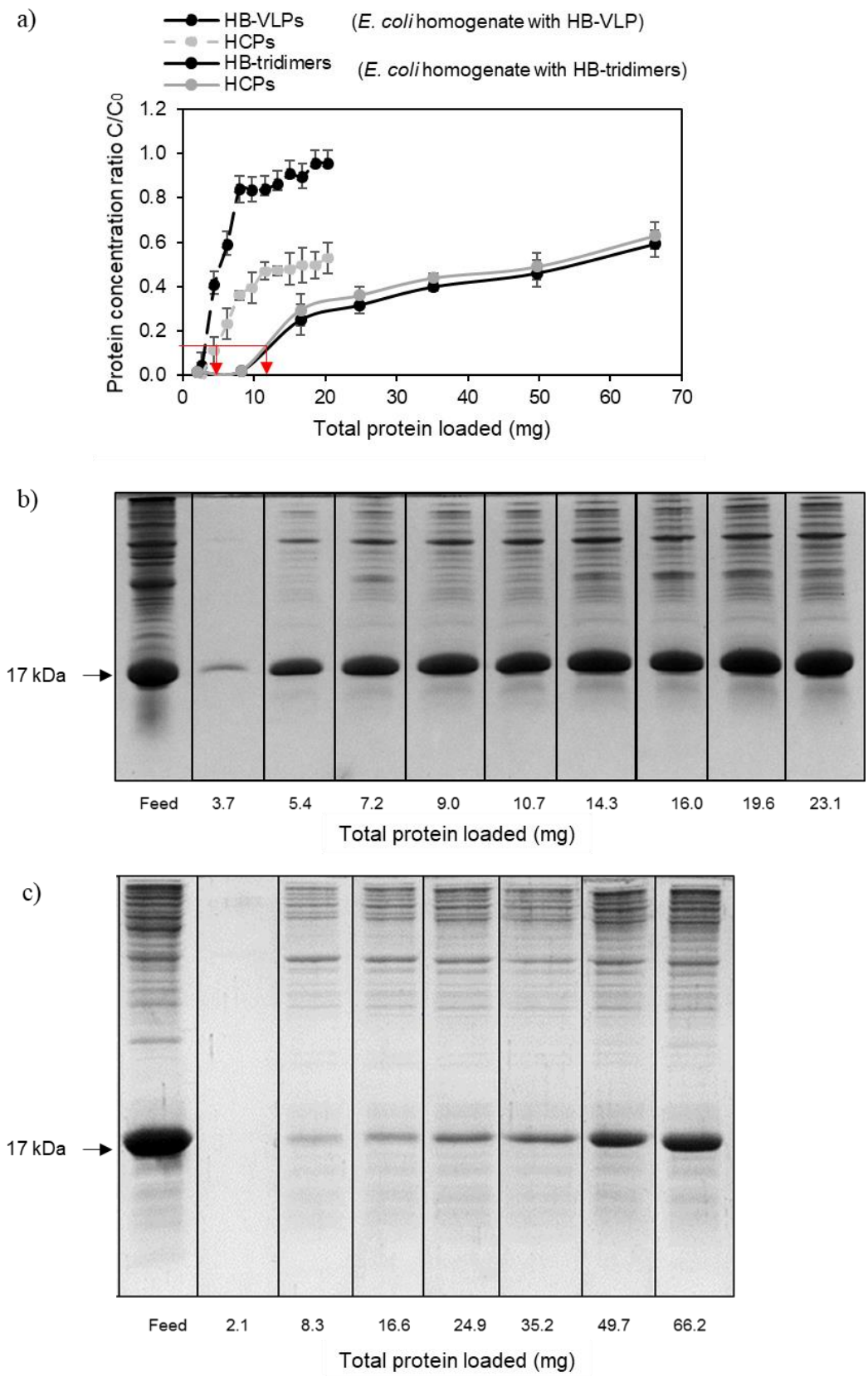

Figure 3. (a) Flow-through protein concentration ratio, C/C_0 with at increasing protein load with respect to the feedstock. SDS-PAGE fractions collected from (b) *E. coli* homogenate containing HB-VLPs and (c) *E. coli* homogenate containing HB-tridimers

The breakthrough curve in Figure 3(a) obtained for *E. coli* homogenate containing HB-tridimer is a typical characteristic of porous diffusive adsorbent – 10% breakthrough of the protein was achieved with relatively low protein load followed by a slow increase in concentration ratio (C/C_0) [84]. In bind-and-elute mode, feedstock are commonly loaded at 10% breakthrough to minimise loss of target protein. The principle can also be applied in FC mode, where 10% HCPs protein breakthrough can be used as an indication of the impurities removal capacity of the adsorbent. Thus, protein load at 10% HCPs breakthrough can be used to indicate a sufficiently high purity product, as most HCPs are adsorbed.

As shown in Figure 3(a), 10% HCPs breakthrough was achieved at 5.5 mg total protein/ml adsorbent for HB-VLPs compared to 13.0 mg total protein/ml adsorbent for HB-tridimers. Besides, breakthrough curve for HB-VLPs and its HCPs are much steeper compared to their HB-tridimers counterpart. This was also observed from the SDS-PAGE results in Figure 3(b), feedstock with HB-VLPs increases drastically and then stabilize at a relatively constant HB-VLPs purity. In contrast, there is a more gradual increase of HB-tridimers purity with protein load [Figure 3(c)]. From the comparison of the two feedstocks, it is apparent that the large HB-VLPs has hindered the adsorption of both HB-VLPs ad HCPs onto the adsorbent. This may be due to the repulsion of HCPs by the HB-VLPs adsorbed on the external surface of adsorbent [5], as well as convective entrapment of the VLPs within the narrow pores [89].

Besides, high protein load did not yield better selective exclusion of the HB-VLPs. As depicted in Figure 3(a), the difference between C/C_0 value of HB-VLPs and its HCPs was 0.29 at 10% HCPs breakthrough. Beyond that, this value increased and maintained at approximately 0.4, i.e. the adsorbent did not show increasing selectivity beyond 10% HCPs breakthrough. In contrast, perfusive adsorbents that possess large µm range pores have shown to exhibit partial displacement at high protein loading [84]. The partial displacement of weakly adsorbed HB-VLPs by HCPs in this study were minimal, it is likely that repulsion effect of adsorbed HB-VLPs prevents diffusion and adsorption of other incoming proteins, that in turn suppresses the desirable displacement effect.

In short, the large size of HB-VLPs was shown to reduce the capacity of the adsorbent to remove HCPs. In addition, loading up to 7.2 mg total protein/ml adsorbent (15 % HCPs breakthrough) can be performed without significant offset to the flow-through purity [from Figure 3 (b)] for standard diffusive adsorbent Sepharose Q FF.

3.3.2. Optimum protein load for FC using POEGMA grafted adsorbent

Since the D_H of HB-VLPs at 30 nm [obtained from Transmission Electron Microscopy (TEM)] [63] is smaller than the adsorbent's pore size (50-70 nm), HB-VLPs may still able to diffuse into the inner part of the adsorbent. To further improve the flow-through recovery of HB-VLP, the anion exchange adsorbents were grafted with POEGMA. However, the size exclusion effect of POEGMA grafts can be affected by the protein load. Therefore, comparison of the breakthrough curves between grafted and ungrafted adsorbent was performed.

At low protein load, more VLPs were excluded by POEGMA grafted QFF-P200 compared to control QFF-C (Figure 4), especially at 5.5-7.0 mg total protein/ml adsorbent. The competitive binding between different proteins the steric hindrance provided by the grafted POEGMA, resulting in a modest difference between grafted and ungrafted adsorbent at higher protein load. Additionally, less HB-VLPs are collected in the flow-through of grafted adsorbent at higher loading, likely caused by interaction with the POEGMA grafts as the amount of adsorbed protein accumulates.

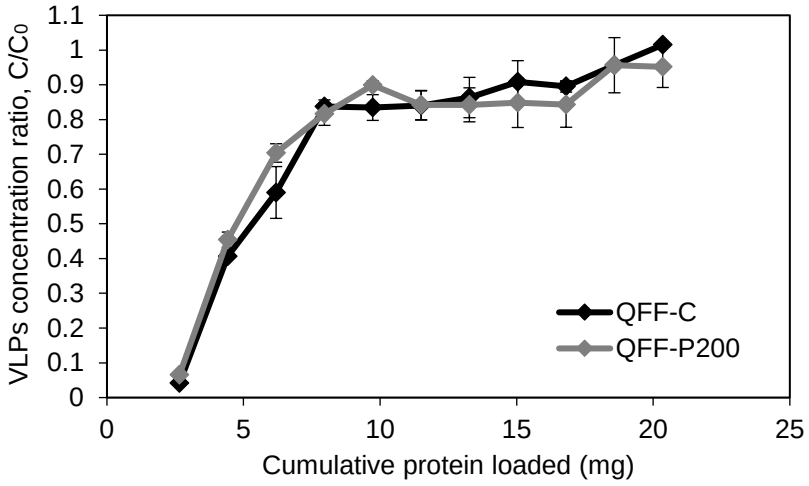

Figure 4. Breakthrough curves for VLPs from *E. coli* homogenate containing HB-VLPs using POEGMA grafted adsorbent

In short, the applicability of POEGMA modified Sepharose Q-FF are not suited at higher protein loading. Hence, all further investigation of FC of feedstock containing HB-VLPs was performed at total protein load of 5.5 mg/ml adsorbent – equivalent to 15% HCPs breakthrough.

3.3.3. Chromatography of *E. coli* homogenate containing HB-VLPs or HB-tridimers

For FC study, the two feedstocks were loaded at approximately 10% HCPs breakthrough, with *E. coli* homogenate containing HB-VLPs at 5.8 mg total protein/ml adsorbent, while *E. coli* homogenate containing HB-tridimers at 12.0 mg total protein/ml adsorbent.

From the results of dynamic light scattering shown in Figure 5(a), the collected flow-through fractions of POEGMA grafted adsorbent contain larger protein compared to the ungrafted adsorbent. This revealed that the grafted adsorbent was effective at size-selective exclusion of HB-VLPs from *E. coli* homogenate. The grafted polymer is responsible for selectively excluding large HB-VLPs from *E. coli* homogenate, with an 10.1% increase of HB-VLPs flow-through recovery, as shown in the corresponding Figure 6(a). Similarly, for *E. coli* homogenate containing HB-tridimers, the flow-through fraction of POEGMA grafted adsorbent also contain larger protein [Figure 5(b)]. However, it was accompanied by an increase in HCPs - a 28.5% rise compared to QFF-C, as shown in Figure 6(b). This is likely caused by a fraction of HCPs that was excluded due to its larger size, implying that HCPs size is not homogenously small. These large HCPs are also excluded with the HB-VLPs, and was expected to reduce the purity of HB-VLPs in the flow-through.

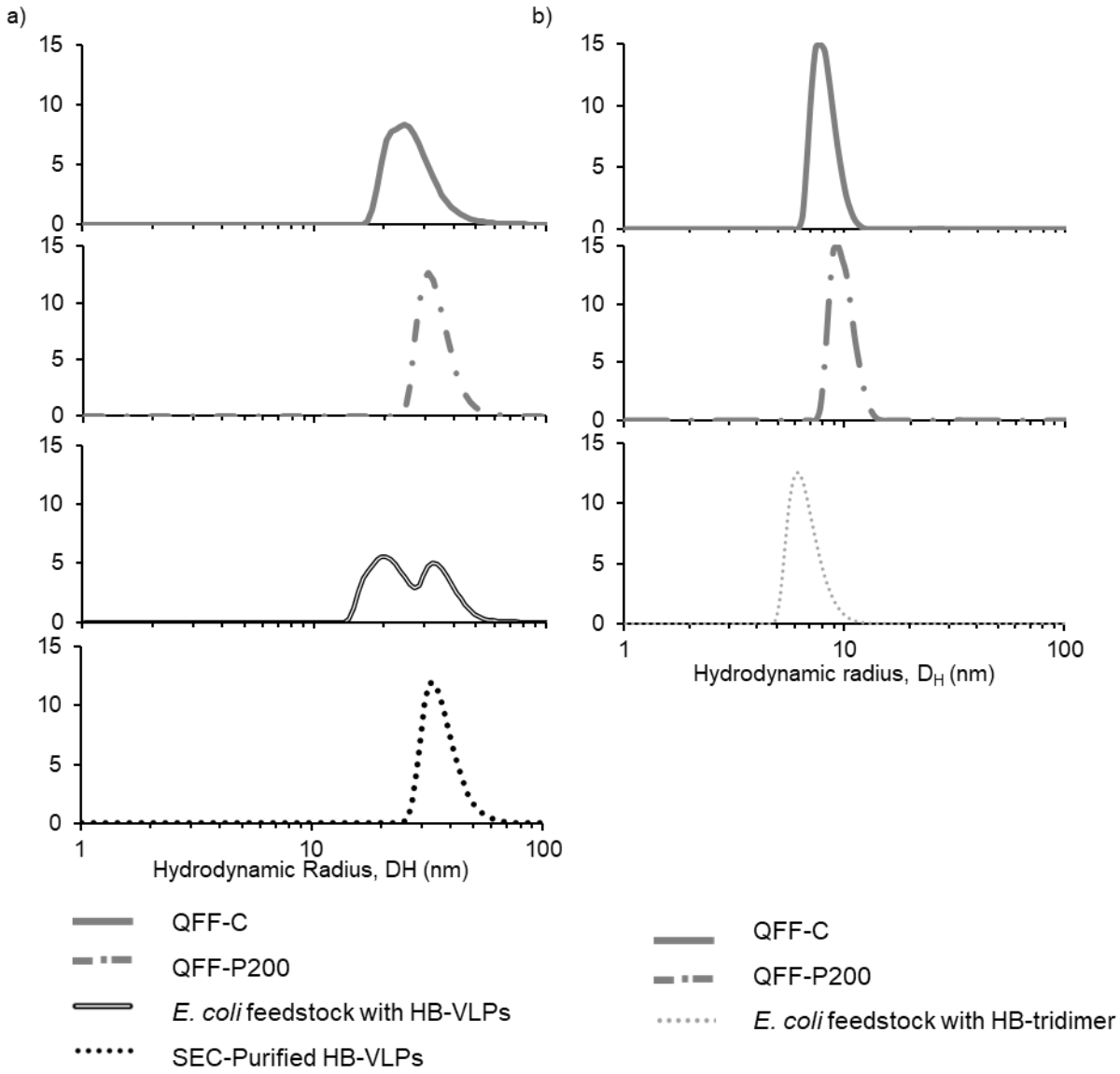

Figure 5. Protein size distribution of the following: (a) flowthrough fraction of (▬) QFF-C, and (▬ ▪ ▬) QFF-P200 after FC of *E. coli* homogenate containing HB-VLPs, (═) *E. coli* homogenate containing HB-VLPs and (••••••) SEC-purified HB-VLPs while (b) flowthrough fraction of (▬) QFF-C, and (▬ ▪ ▬) QFF-P200 after FC of *E. coli* homogenate containing HB-tridimers and (·····) *E. coli* homogenate containing HB-tridimers

As shown in Figure 6, a significant difference between the amount of HB-VLPs and HB-tridimers collected in the flow-through fraction was observed; with 80% of HB-VLPs collected in flow-through while only 10% of HB-tridimers was collected. HCPs removal from feedstock with HB-tridimers was also much higher at 4.5 mg HCPs/ml adsorbent while only 1.0-1.6 mg

HCPs/ml adsorbent was adsorbed from feedstock with HB-VLPs. The results from FC were consistent with the results of breakthrough curves using high protein load.

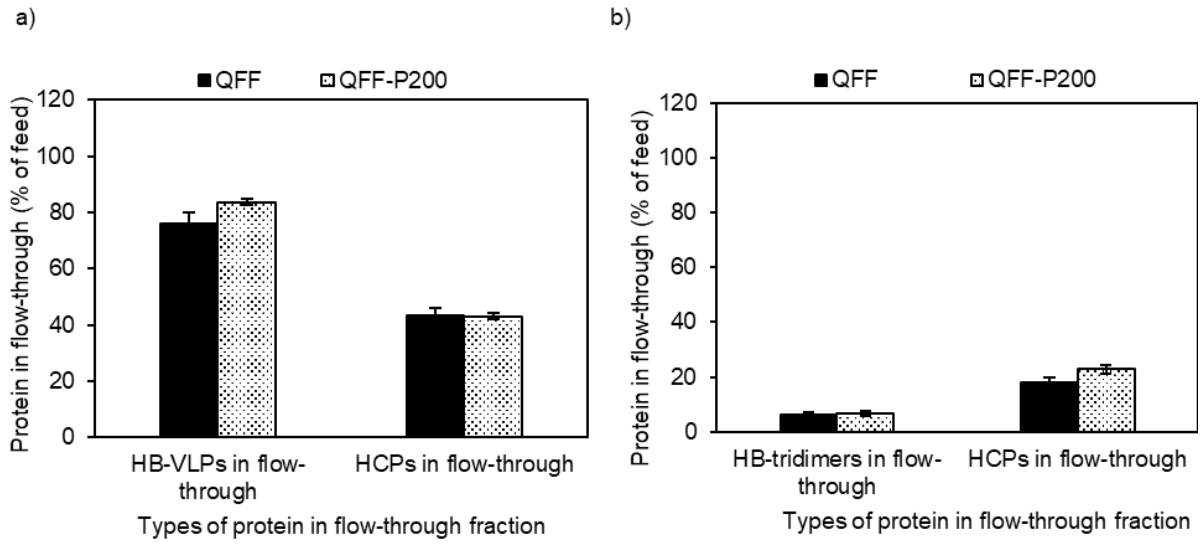

Figure 6. Protein collected in the flow-through fraction of (a) *E. coli* homogenate containing HB-VLPs and (b) *E. coli* homogenate containing HB-tridimers

In short, FC results are mostly similar to results from previous section with feedstock containing HB-VLPs excluded significantly more by the adsorbents compared to HCPs. Besides, comparison between the two feedstock have shown presence of large HCPs can also flow-through along with the target HB-VLPs. These large HCPs are likely to be responsible for a reduced HB-VLPs purity in the product.

3.3.4. Effect of protein size on adsorption of HB-VLPs and HB-tridimers under batch condition

CLSM images in Figure 7 show the distribution of FITC-labelled HB-VLPs and FITC-labelled HB-tridimer on the two anion-exchange adsorbents after 6 h batch adsorption. The FITC-labelled HB-tridimer can be clearly observed to have diffused into the pores of both

adsorbents. Due to its small size, the diffusion of HB-tridimers was not affected by the grafted POEGMA, resulting in similar distribution between adsorbents shown in Figure 7(a) and Figure 7(b).

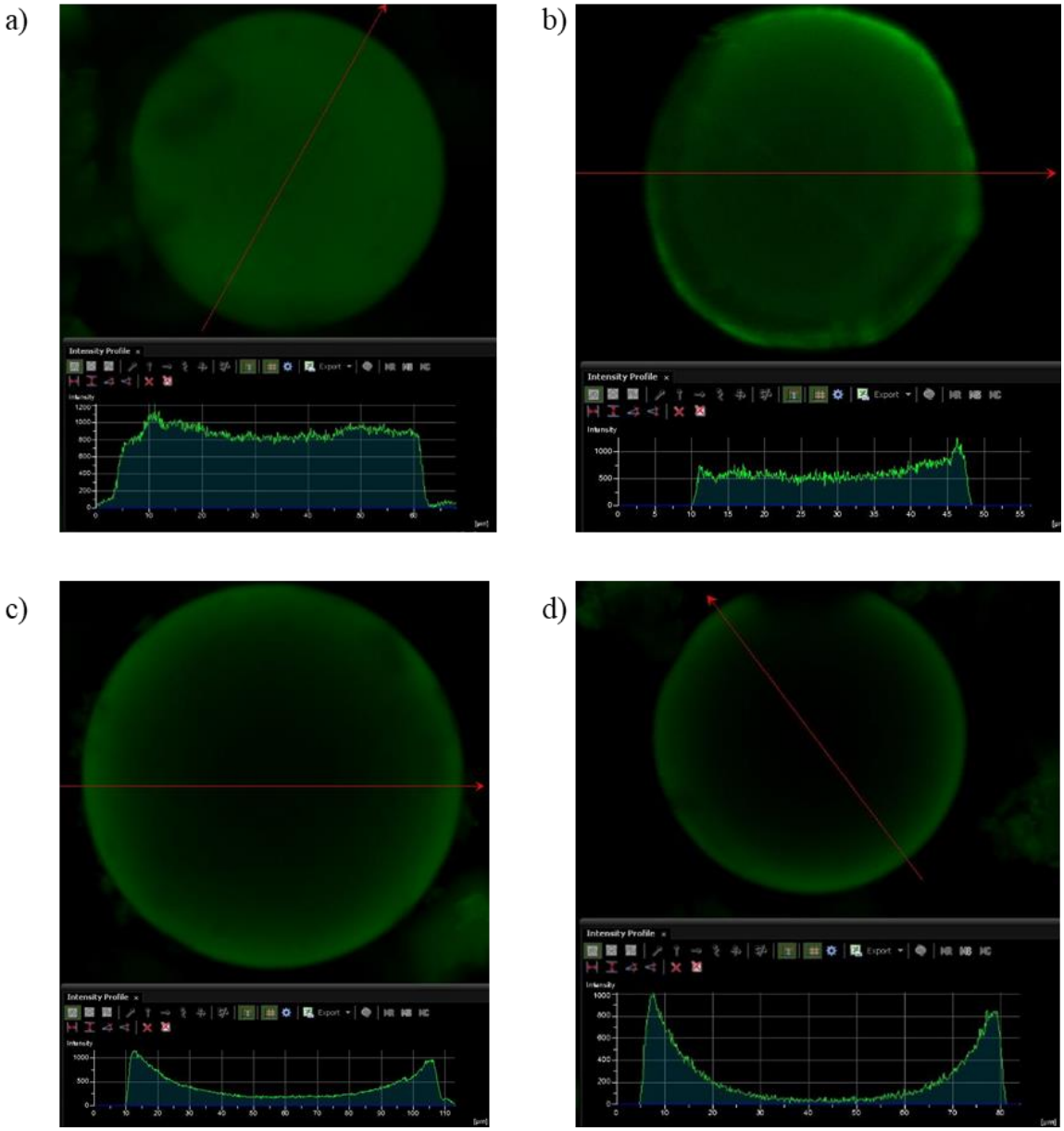

Figure 7. Confocal laser scanning microscopy (CLSM) of FITC-labelled HB-tridimer on (a) ungrafted QFF-C, (b) polymer grafted QFF-P200; FITC-labelled HB-VLPs on (c) ungrafted QFF-C, (d) polymer grafted QFF-P200 after batch adsorption

Conversely, the CLSM results showed that the adsorption of HB-VLPs on both adsorbents was mostly confined to the external surface of the adsorbents, as diffusion of large VLPs have been shown to be limited to external surface area on standard diffusive adsorbents [5]. Nonetheless, from Figure 7(d), POEGMA grafted adsorbent has slightly reduced the diffusion of HB-VLPS, with a visibly thinner and more confined layer of HB-VLP_S on the external surface of the QFF-P200 adsorbent. Even though batch condition was not a perfect representation of flow condition of FC, the CLSM results provides qualitative validation of the FC results, verifying that large HB-VLPs and HCPs have lower adsorption and are confined to binding sites on the external surface of the adsorbent.

3.3.5. Applicability of grafted POEGMA on exclusion of MrN-VLPs

The hydrodynamic radius of MrN-VLPs estimated from TEM is approximately 30 nm [90], similar to HB-VLPs. The high expression of HB-VLPs from *E. coli* has allowed us to modify diffusive anion exchange adsorbent for initial isolation step. Unlike HB-VLP, *Macrobrachium rosenbergii* nodavirus like particles (MrN-VLPs) expressed with *E. coli* usually results in clarified homogenate of around 7 % purity, as shown in lane 1 (at 51 kDa) of Figure 7(b). [13]. In contrast, *E. coli* homogenate contained HB-VLPs (35 % purity). The low purity of *E. coli* homogenate containing MrN-VLPs makes it ill-fitted to be purified using FC. However, FC of this feedstock allows evaluation of the size selective exclusion of VLPs from a feedstock with lower VLP purity.

QFF-C adsorbent showed a flow-through recovery of 19.0% while QFF-P200 showed recovery of 33.8 % (a 78.0% increase), as shown in Figure 7(a). The difference of MrN-VLPs purity obtained in the flow-through fraction is apparent in lane 2 and lane 3 in Figure 7(b). Due to low VLP purity of the *E. coli* homogenate, the repulsion caused by the VLPs adsorbed on the external surface of the adsorbent is considerable lower. This in turn results in a more

prominent effect by the grafted POEGMA, resulting in a significant increase in VLPs flow-through recovery.

However, the PF was expectedly low (0.63 for QFF-C and 0.90 for QFF-P200), as well as the flow-through recovery. As FCs are generally tailored for feedstock with higher purity of VLPs, emphasis should be on the protein load. Nonetheless, further optimisation should be performed to determine the better flow-through recovery and PF.

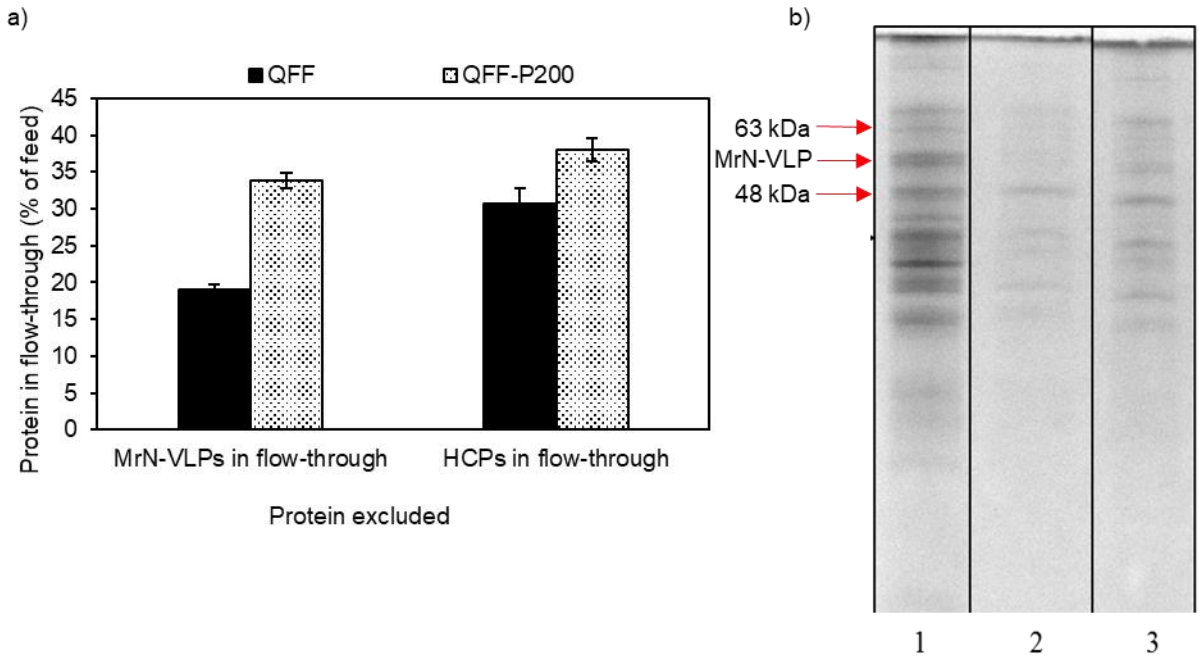

Figure 8. (a) MrN-VLPs and its HCPs collected in the flow-through fraction and (b) SDS-page results with Lane 1, *E. coli* homogenate containing MrN-VLPs; Lane 2, flow-through pool of QFF-C; Lane 3, flow-through pool of POEGMA grafted Sepharose QFF (QFF-P200)

3.4. Conclusion

From the above results, investigation of protein size effect showed that HB-VLPs reduced the overall adsorption capacity of the adsorbent. Dynamic light scattering analysis of flow-through fraction indicate that large HCPs that cannot be adsorbed are likely to be responsible for limiting higher HB-VLP purity achievable from FC. Compared to other VLPs from *E. coli* homogenate, *E. coli* homogenate containing HB-VLPs are uniquely suited for FC at initial isolation step due to its high protein concentration (10 mg total protein/ml) and VLPs purity (37 % HB-VLPs). In short, the optimum range of protein load of *E. coli* feedstock containing HB-VLPs has been determined to be around 5.5 – 7.0 mg total protein/ml adsorbent (15% HCPs breakthrough). Further optimisation on the adsorbent design will be based on this protein load.

Chapter 4: Size-selective purification of hepatitis B virus-like particle in flow-through chromatography: types of ion exchange adsorbent and grafted polymer architecture

4.1. Introduction

In FC of VLPs, the impurities are adsorbed on the adsorbent while the target VLPs are recovered in the flow-through fractions [85]. This mode of operation circumvents the shortcomings of bind-and-elute (BE) mode of chromatography, such as the low adsorption capacity of adsorbents and the risk of VLP disassembly. However, widespread application of FC for the recovery of VLPs and viruses [10,12,31,91] is still uncommon, mainly due to the lack of versatile commercial FC adsorbents.

Poly[oligo(ethylene glycol) methyl ether methacrylate] (POEGMA) is a type of anti-fouling polymer. Capitalizing on its ability to resist protein adsorption, our group has developed POEGMA-grafted ion exchange adsorbents (Sepharose QFF) for FC of HB-VLPs [64]. Reduction of HB-VLPs adsorption was achieved while adsorption of smaller HCPs (approximately 5 nm [92]) was held relatively constant when POEGMA grafted adsorbents were used. The interaction between target protein (i.e., HB-VLPs) and positively charged quaternary ammonium ligands (Q ligand) have been shown to be modulated by controlling the chain length of polymer grafted on the absorbent [64].

Nevertheless, the FC recovery of viruses and VLPs could be improved further by reducing the accessible binding site of the adsorbent. Large anion exchange adsorbent (200 μm) have been shown to reduce the undesired adsorption of influenza viruses on the external surface of FC adsorbents [31]. Charged dextran grafts have also shown an improved adsorption of small HCPs while being restrictive to large biomolecules [93]. Q Sepharose XL, a type of commercial adsorbent grafted with charged dextran, has been successfully used for the initial isolation step in FC mode to purify influenza virus [91]. Besides, the size exclusion effect caused by the POEGMA branch chain was not fully explored. As the length of branch chain of polymer was known to affect the antifouling properties of modified surfaces [74], it is postulated that a stronger size exclusion effect could be achieved by optimizing the branch chain length POEGMA grafts.

The 2nd phase of the project aimed to further investigate the role of inert POEGMA graft on the size-selective purification of HB-VLPs by ion exchange adsorbents (i.e., Sepharose family). Firstly, the effect of adsorbent size (and the accessible binding sites) on the FC performance was evaluated. Besides, the size exclusion effect of the ethylene oxide branch-chain length of POEGMA grafts was not fully explored in previous studies [14,63]. It is postulated that a stronger size exclusion effect could be achieved by optimizing the length of ethylene oxide branch-chain of POEGMA grafts. Finally, the role of POEGMA grafts in reducing strong multipoint adsorption and the resulting effect on HB-VLPs assembly were evaluated. POEGMA grafts and dextran grafts of Q Sepharose XL adsorbents were also compared to evaluate the effect of functionality of polymer grafts on FC performance.

4.2. Materials and Methods

4.2.1. Chemicals and materials

Anion exchange agarose adsorbents, namely Q Sepharose FF, Q Sepharose XL and Q Sepharose High Performance, were purchased from GE Healthcare (Switzerland). Monomers including di(ethylene glycol) methyl ether methacrylate (MEO_2MA), poly(ethylene glycol) methacrylates of M_n=300 ($OEGMA_{300}$) and M_n=500 ($OEGMA_{500}$) were sourced from Sigma-Aldrich (Singapore). Prior to the polymerization reaction, the monomers were purified with a neutral alumina flash chromatography. Ammonium persulfate (APS), silver nitrate ($AgNO_3$) and ammonium sulfate were sourced from Acros Organics (Geel, Belgium). Protein assay dye reagent concentrate was purchased from Nacalai Tesque (Japan).

4.2.2. Preparation of clarified *E. coli* homogenate containing HB-VLPs

As outlined in section 3.2.2, *E. coli* homogenate containing HB-VLPs was prepared from *E. coli* cells (W31101Q strain) and subsequently harvested and clarified.

4.2.3. Preparation of HB-VLPs purified with size exclusion chromatography (SEC)

SEC-purified HB-VLPs stock was prepared according to protocol described by Yoon et al. [13]. Briefly, ammonium sulfate precipitation was performed before size exclusion chromatography. Ammonium sulfate was added to 35% saturation and stirred at 4˚C for 2 h. The precipitated proteins were recovered by centrifugation at 18, 000 g at 4˚C for 30 min. The pellet containing the HBcAg was resuspended in 50mM Tris-HCl, 100 mM NaCl (pH 8) buffer, and dialyzed against the same buffer with two changes. 2 ml of the processed homogenate was then purified with size exclusion chromatography (SEC) using Sephacryl-500 adsorbents in a XK 16/100 column (GE Healthcare) on the Akta Purifier system. The column was equilibrated with 50 mM Tris-HCl, 100 mM NaCl (pH 8) prior to loading. Proteins were resolved using a flow rate of 0.5 ml/min and fractions containing HB-VLPs were collected. Purity of HB-VLPs obtained were 92%. The final concentration of SEC-purified HB-VLPs was adjusted by dilution with 50mM Tris-HCl, 100 mM NaCl (pH 8) buffer and confirmed with Bradford Assay.

4.2.4. Instruments and apparatus

Eutech Instrument PC700 (USA) was used to measure conductivity of the adsorbent in adsorbent-water mixture. The functional groups on the polymer grafted agarose beads were evaluated with an attenuated total reflectance-Fourier transform infrared (ATR-FTIR) spectrometer (Thermo Scientific, model Nicolet^{TM} iS10 FT-IR, USA). A thermogravimetric analyzer (TA Instruments, model Q50 TGA, USA) was used to assess the amount of grafted POEGMA with respect to the unmodified adsorbents. A particle size analyzer (Malvern, model Zetasizer Nano ZS, UK) equipped with He-Ne laser (633 nm) was used to determine the size distribution of proteins. The FC of clarified *E. coli* homogenate was performed using a fast

protein liquid chromatography system (GE Healthcare, model AKTA Purifier 10, UK). The chromatogram was recorded at wavelength 280 nm.

4.2.5. Grafting of POEGMA on anion exchange adsorbents

The free radical graft polymerization of POEGMA polymer on different adsorbents was performed according to the steps outlined in Section 3.2.4. However, the pre-purged monomer solution (MEO_2MA, $OEGMA_{300}$ or $OEGMA_{500}$) used was shown in Table 2, with the same monomer ratio of 2 mmol monomers to 2 g adsorbent. After the reaction, the adsorbents were washed with a copious amount of deionized water.

Table 2. Modified adsorbents and their respective polymerization conditions. Reaction performed under nitrogen at 60ºC for 3 h with ammonium persulfate as the initiator

Type of unmodified adsorbent	Abbreviation	Monomer ratio
Q Sepharose FF	QFF-C (Control)	-
	QFF-P200	90% MEO_2MA 10% $OEGMA_{300}$
	QFF-P300	100% $OEGMA_{300}$
	QFF-P500	100% $OEGMA_{500}$
Q Sepharose XL	QXL-C (Control)	-
	QXL-P200	90% MEO_2MA 10% $OEGMA_{300}$
Q Sepharose High Performance	QHP-C (Control)	-
	QHP-P200	90% MEO_2MA 10% $OEGMA_{300}$

4.2.6. Characterization of POEGMA-grafted adsorbent

FTIR spectroscopy was performed to qualitatively confirm the POEGMA grafted on the adsorbents. To evaluate the amount of POEGMA grafted on adsorbent, thermogravimetric analysis (TGA) was performed. In brief, the oven-dried adsorbent was heated to 750°C at 10°C/min under nitrogen. The weight losses in adsorbent at 150°C and 700°C were recorded [85]. The % weight of grafted POEGMA on the modified adsorbent with respect to the unmodified adsorbent was calculated using Eq. 4-1:

$$\%\ \text{weight of grafted POEGMA} = (\mathrm{W}_{f,c} - \mathrm{W}_{f,i}) \times 100\% \qquad \text{(Eq. 4-1)}$$

where W_f is the final weight fraction of absorbent at 700°C; the subscripts *i* and *c* represent the type of modified adsorbent and its respective control (type of unmodified adsorbent).

The ionic capacity of the unmodified adsorbents were characterized by conductometric titration method according to the protocol used by a previous study [85]. Briefly, 0.01 M of silver nitrate ($AgNO_3$) was added to a mixture of 0.1% (w/v) of Q adsorbent with a step size of 0.1 ml. The conductivity of the mixture was measured with Eutech Instrument PC700 (USA) every 3 min. The conductivity increases gradually until the titration was completed, which was indicated by a sharp increase in the measured conductivity. The ionic capacity (mmol Cl^- /ml adsorbent) of the adsorbent is equal to the amount of $AgNO_3$ (mmol) added per unit volume of adsorbent.

4.2.7. Flow-through chromatography of *E. coli* homogenate and chromatography of SEC-purified HB-VLPs

Similar to Section 3.2.5., the FC of HB-VLPs was performed with a fast protein liquid chromatography system. Following the protocol provided by the supplier (BioToolomics, United Kingdom), the column was slurry-packed with adsorbents to a volume of 1.0 ml. First, the column was equilibrated with 5 ml of Buffer A (25 mM Tris–HCl; pH 8.0). Next, 0.5 ml of feed [clarified homogenate (5.8 mg of total proteins and 35.5 – 37.0 % of HB-VLPs)] was loaded to the packed column. Then, 2.5 ml of Buffer A was flowed through the column. Next, the column was flushed with 0.2 ml of Buffer A to wash off the unbound proteins. Lastly, an isocratic elution was performed using Buffer B (11 ml; 25 mM Tris–HCl; pH 8.0; 1 M NaCl).

A similar protocol was used for the chromatography of SEC-purified HB-VLPs. However, 0.5 ml of SEC-purified HB-VLPs with protein concentration of 1 mg/ml at 92% purity was injected (loaded).

4.2.8. Quantification of protein

For SEC-purified HB-VLPs, the ratio of flow-through and eluted protein with respect to total protein loaded was determined from the area under curve of the chromatograms.

For FC using *E. coli* feedstock, protein concentration of collected fractions was determined using the Bradford assay [86]. The purity of HB-VLPs of a collected fraction was evaluated using sodium dodecyl sulfate-polyacrylamide gel electrophoresis (SDS-PAGE) as outlined in section 3.2.6. [87]. The purity of HB-VLPs was determined as the ratio of the intensity of the HBcAg band to that of all the protein bands, as described by Tey et al. [75].

4.3. Results and Discussion

4.3.1. Characterization of adsorbents

The presence of polymer graft on the modified adsorbents was confirmed qualitatively by ATR-FTIR analysis. As shown in Figure 9, the characteristic stretching vibration of the carbonyl group (C=O) at 1730 cm^{-1} indicates the presence of POEGMA on the following modified adsorbents: QFF-P200, QFF-P300, QFF-P500, QXL-P200, and QHP-P200.

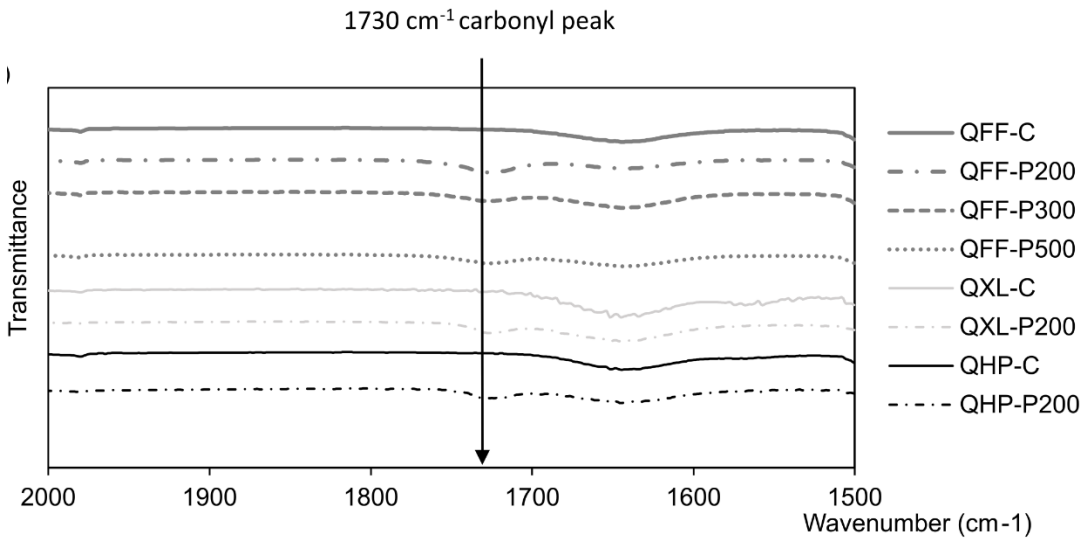

Figure 9. FTIR spectra of the following adsorbents: (——) QFF-C, (— · ·) QFF-P200, (- - -) QFF-P300, (·····) QFF-P500, (———) QXL-C, (· · · ·) QXL-P200, (- · —) QHP-C, (—) QHP-P200.

Based on Table 2, the % weight of POEGMA grafted for QFF-P500 adsorbent with respect to the control adsorbent QFF-C was lower than the % weights of QFF-P200 and QFF-P300. This indicated a lower amount of POEGMA grafted on QFF-P500 adsorbent. On the other hand, QXL-P200 adsorbent, which was pre-grafted with charged dextran, exhibited a higher amount of POEGMA grafted compared to QFF-P200. The grafting of POEGMA requires hydroxyl group as the initiating site for polymerization. The hydroxyl groups on the

dextran grafts of QXL-P200 adsorbent resulted in a higher overall number of accessible hydroxyl groups for initiation and consequently a higher amount of POEGMA grafted.

As shown in Table 3, the % difference weight of QFF-P200 adsorbent was lower than that of QHP-P200 adsorbent. This is because the larger adsorbent possess a lower amount of accessible site for initiation and polymer growth, which in turn caused a lower amount of polymer grafted.

The charged dextran grafts on QXL and the smaller size of QHP leads to more accessible binding sites and resulted in a higher ionic capacity (ligand density) measured. Meanwhile, the grafting of POEGMA on three types of adsorbents only slightly changed ionic capacity as measured using silver nitrate titration method (Table 3).

Table 3. Ionic capacity of adsorbents and the TGA results of modified adsorbents with respect to its unmodified controls

Adsorbent	Adsorbent size[a] (μm)	Ionic capacity[b] (mmol Cl- / g adsorbent)	% difference weight loss
QFF-C	90	0.092	-
QFF-P200	90	0.091	3.33
QFF-P300	90	0.089	3.73
QFF-P500	90	0.089	1.93
QXL-C	90	0.271	
QXL-P200	90	0.266	12.42
QHP-C	35	0.247	
QHP-P200	35	0.239	10.29

[a] According to manufacturer's data

[b] From titration of $AgNO_3$

4.3.2. Effect of adsorbent size on HB-VLPs adsorption

The chromatography of SEC-purified HB-VLPs using adsorbents with different sizes was conducted. As both are standard diffusive adsorbents with similar pore size of 50-100 nm (with exclusion limit [Mr] [Globular Proteins] of $4x10^6$ Da) [94–96], the larger adsorbents are

expected to show a low adsorption of HB-VLPs, and are likely to have a better flow-through recovery of HB-VLP from *E. coli* homogenate in FC.

From Figure 10(a), it can be observed that the smaller QFF-C showed a higher flow-through of SEC-purified HB-VLPs as compared to the larger QHP-C. Similarly, the FC of *E. coli* homogenate using QFF-C demonstrated a higher flow-through recovery [approximately 2 fold; as shown Figure 10(b)]. The larger adsorbent size of QFF-C resulted in a less accessible binding sites which consequently reduced undesired adsorption of HB-VLPs and improved its flow-through recovery.

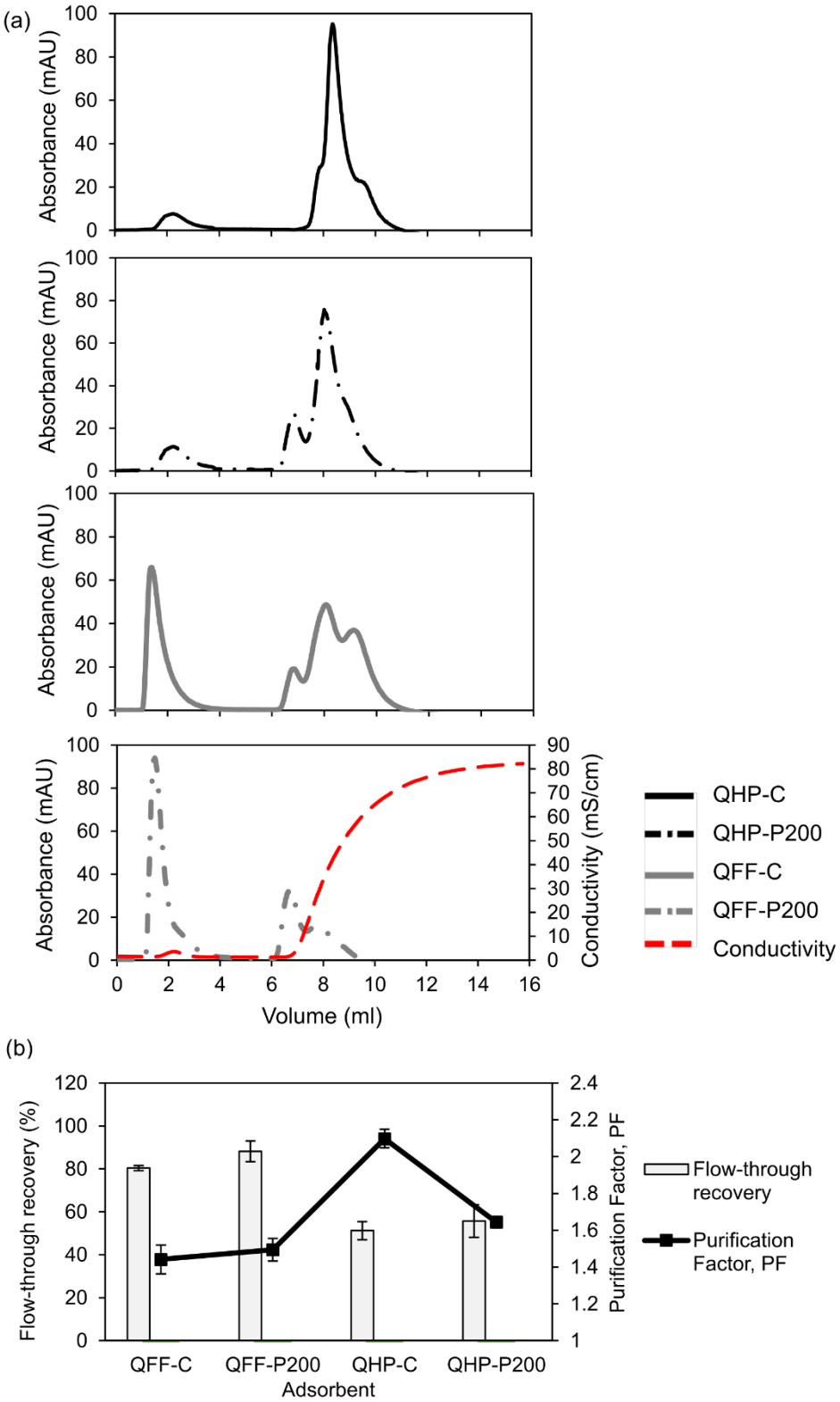

Figure 10. (a) Chromatograms of SEC-purified HB-VLP feedstock using adsorbents with different size: QHP-C (35 µm) and QFF-C (90 µm), with QHP-P200 and QFF-P200 representing the respective adsorbent grafted with $POEGMA_{200}$. Absorbance (mAU) for (——) QHP-C, (-·-) QHP-P200, (——) QFF-C, and (– · ·) QFF-P200; and (— —) conductivity (mS/cm) against volume of buffer (ml) flowed in the column. (b) Flow-through recovery and PF of HB-VLP from *E. coli* homogenate

As the D_H of HB-VLPs [30 nm, as shown in Figure 11(b)] is smaller than the adsorbent's pore size (50-100 nm), the anion exchange adsorbents were grafted with POEGMA to further reduce unwanted adsorption of HB-VLPs. As shown in Figure 10(a), the QFF-P200 adsorbent (with $POEGMA_{200}$ grafts) showed a higher flow-through of SEC-purified HB-VLPs, in comparison to its ungrafted control (QFF-C). As such, QFF-P200 successfully reduced the HB-VLP in FC mode, thereby giving the higher recovery and PF of HB-VLPs (as shown in Figure 10(b)). However, a significant drop of PF was shown for smaller QHP-P200, likely caused by the high amount of POEGMA grafted (as shown in Table 3), which in turn result in excessive diffusional resistance on HCPs. This leads to an undesired reduction in HCPs adsorption, lowering the flow-through PF. Other example of excessive resistance to protein diffusion in agarose-coated FC adsorbents was also reported [63].

The effect of POEGMA on adsorption SEC-purified HB-VLPs can be observed in Figure 10(a) - lower amount was eluted at a higher conductivity, indicating a reduction in strong multipoint adsorption of SEC-purified HB-VLP on the adsorbent, that have been shown to cause disintegration of VLPs as reported by Huang et al. [32]. Dynamic light scattering results based on particle size's volume distribution in Figure 11(b) showed that QHP adsorbents with high capacity (high ligand density) caused most of the eluted HB-VLPs to disintegrate (the size of the eluted proteins are less than 10 nm). In comparison, the proteins eluted from QFF-C and QFF-P200 contain significantly more intact HB-VLP (protein in the 10-30 nm range). Additionally, eluted fraction of polymer grafted QFF-P200 was found to contain more intact HB-VLP (35%) range compared to its ungrafted control (19%).

As most of the smaller HCPs was adsorbed in FC mode, Figure 11(a) showed that proteins in flow-through fractions (average: 37 nm) were generally larger than the proteins in

the feedstock (46 % average: 21 nm; 54% average: 37 nm) in Figure 11(c). Besides, protein size profile of flow-through fractions of QFF-C and QFF-P200 generally closely resembles the size distribution of SEC-purified HB-VLPs, indicating minimal disassembly of HB-VLPs in the flow-through has occurred. The protein size analysis also showed that the use of QFF-P200 resulted in a flow-through fraction with slightly larger proteins, confirming the role of POEGMA in improving the size-selective effect of QFF.

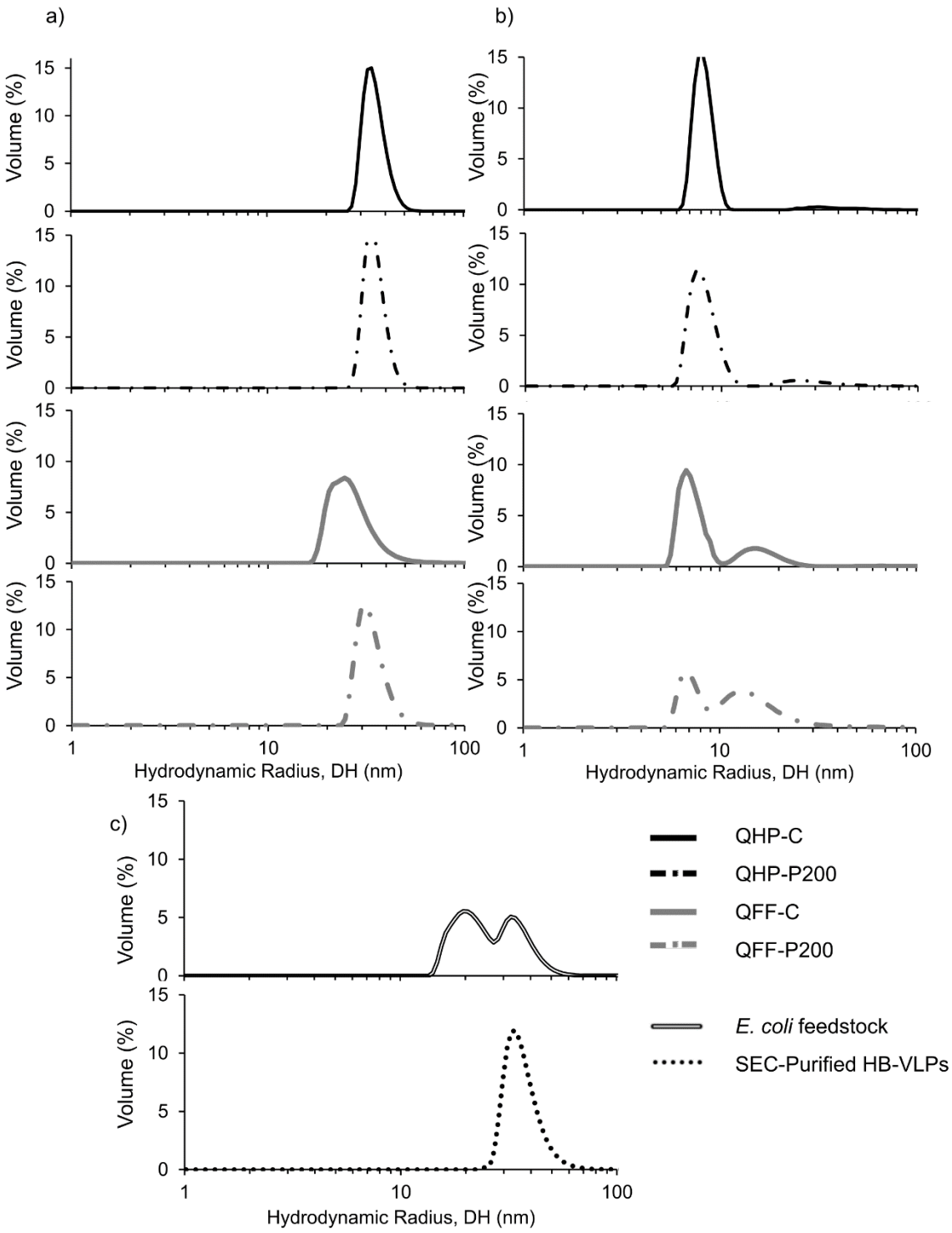

Figure 11. Size distribution in terms of volume based distribution of proteins collected in the a) flow-through fractions, and b) eluted fractions of adsorbents (▬) QHP-C, (▬·▬) QHP-P200, (▬) QFF-C, and (▬·▬) QFF-P200, and c) (═) *E. coli* feedstock and (·····) SEC-purified HB-VLPs.

In general, the QHP-C adsorbent provides a better PF but a low recovery of HB-VLP [Figure 10(b)], indicating that a smaller adsorbent will be ill-suited for an initial capture of clarified feed. Additionally, POEGMA grafted QFF-P200 was shown to effectively reduced disintegration of eluted protein and strongly adsorbed SEC-purified HB-VLPs.

4.3.3. Comparison between charged dextran grafts and POEGMA grafts for FC

Charged dextran grafts grafted on ion exchange adsorbents was known to significantly improve the adsorption capacity of small proteins, while being restrictive towards the large biomacromolecules as it possess significantly smaller apparent pore size [97]. Consequently, the dextran grafts should aid in the exclusion of large HB-VLPs. However, Figure 12 showed that QXL-C adsorbent showed a lower flow-through recovery compared to QFF-P200, with only modest increase in PF. It is likely that the additional binding sites on the charged dextran has increased the adsorption of both HB-VLPs and HCPs.

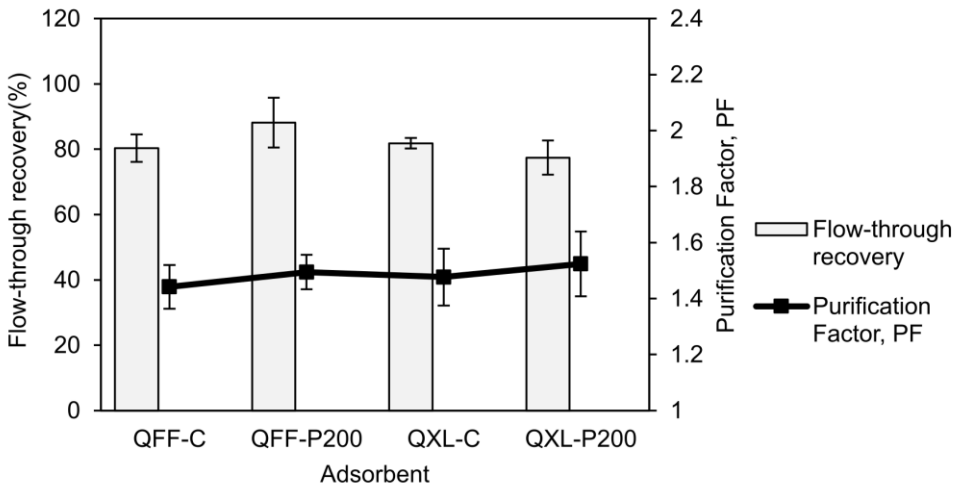

Figure 12. Flow-through recovery and PF of HB-VLP from *E. coli* homogenate using standard adsorbents QFF-C, adsorbents grafted with $POEGMA_{200}$ (QFF-P200), Sepharose XL adsorbents (QXL-C) and POEGMA grafted QXL-P200

As illustrated in Figure 13 , the QXL-P200 adsorbent represents the combined effect of charged dextran and POEGMA grafts on the performance of the adsorbents. As shown in Figure 12, POEGMA grafted on QFF-P200 resulted in better flow-through recovery and PF compared to its control QFF-C. In contrast, the POEGMA on QXL-P200 resulted in a lower (5.3 %) flow-through recovery with its control QXL-C. This could be due to the protein (HB-VLPs) entrapment by the grafted polymer has been reported by Lee et al. [63]. Since much more $POEGMA_{200}$ was grafted on QXL-P200 (Table 3), the restricted pores and the combined dextran and POEGMA grafts could have trapped HB-VLPs and contributed to a lower flow-through recovery and PF.

Despite the smaller apparent pore size of QXL adsorbents, the additional binding sites on dextran grafts affected the flow-through recovery and PF. Based on the current findings, the adsorbent grafted with POEGMA outperformed the adsorbent grafted with dextran, due to POEGMA's non-charged and inert properties.

4.3.4. Effect of the branch chain length of grafted POEGMA

Polymer architecture also plays a pivotal role in reducing the diffusion of larger VLPs to the surface of the POEGMA grafted adsorbents. The length of branch-chain of the grafted POEGMA was varied by using different OEGMA monomers for polymerization. In this study, an increase in the repeating unit of ethylene oxide (branch-chain) was expected to increase the steric hindrances exerted on large protein, such as HB-VLPs.

The improvement of exclusion provided by increasing branch chain length was partially offset by significant reduction in amount of polymer grafted (Table 3). Hence, from Figure 14(a), flow-through recovery and PF of QFF-P300 are only slightly better than QFF-P200. $POEGMA_{500}$ showed a better performance in PF but lower flow through recovery compared to $POEGMA_{300}$. The lower flow through recover obtained in $POEGMA_{500}$ is most probably due to its lower amount of polymer grafted. The longer and more hydrophilic branch-chain forms a thicker hydration layer [74], thus $POEGMA_{500}$ is more effective at reducing the interaction between HB-VLPs and Q ligands as illustrated in Figure 13(b). Optimisation of polymerisation condition could increase the amount of $POEGMA_{500}$ grafted.

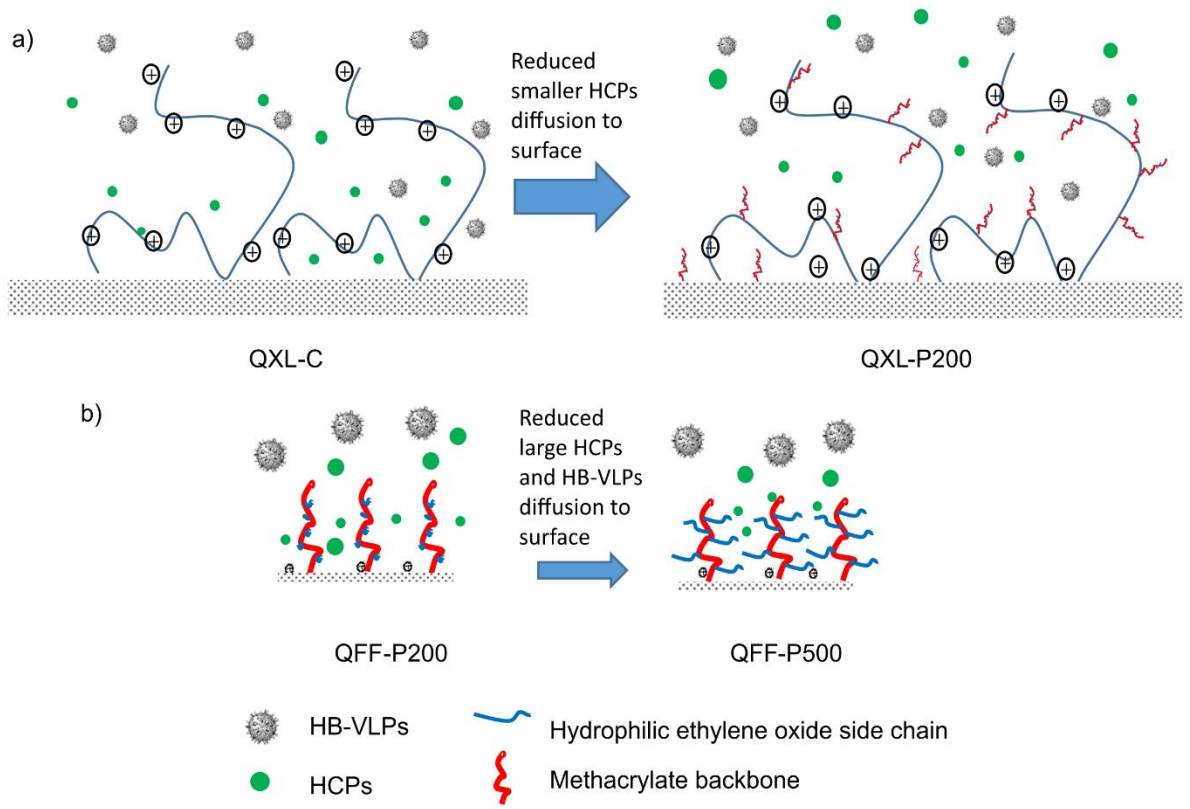

Figure 13. Illustration of size-selective exclusion of the HB-VLPs and the larger HCPs from the external surface of adsorbents. The smaller HCPs are able to approach the external surface and pores in the adsorbent. (a) Adsorption of HB-VLPs on the additional binding sites of grafts on the unmodified Sepharose XL adsorbent (QXL-C); the dense $POEGMA_{200}$ grafts on QXL-P200 adsorbent reduced the diffusion of HCPs to external surface of the adsorbent, and (b) Sepharose Q grafted with POEGMA of increasing side chain length increased the exclusion of larger HCPs and HB-VLPs

Besides, the adsorbents modified with POEGMA (i.e., QFF-P200, QFF-P300 and QFF-P500 adsorbents) showed a modest improvement of PF and flow-through recovery compared to ungrafted control- approximately 5%. As discussed in Section 3.3.3., the limited improvement was likely due to a small but significant fraction of HCPs that were larger in size, causing more HCPs in the flow-through fraction along with the target HB-VLPs that consequently reduces the purity of the flow-through fractions.

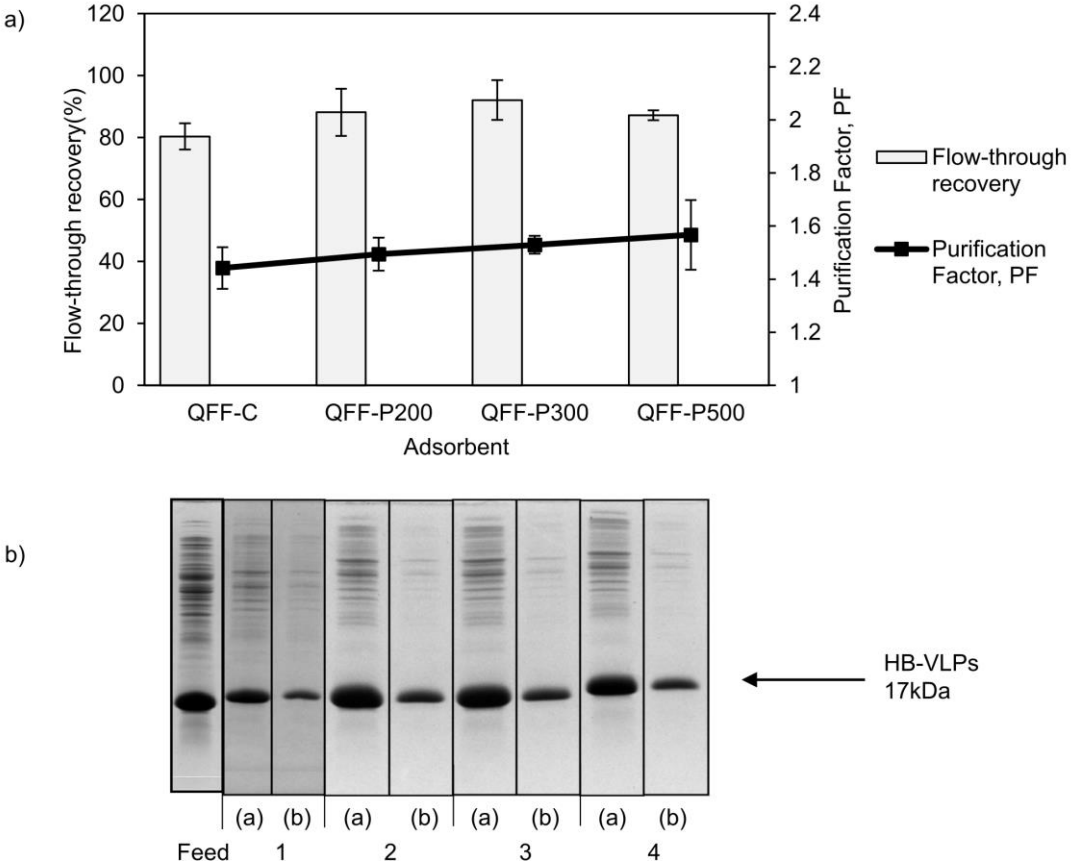

Figure 14. (a) Flow-through recovery and PF of FC of HB-VLPs from *E. coli* homogenate and (b) SDS-PAGE results of the feed and flow-through fractions collected. Lanes 1, 2, 3 and 4 represents the fractions purified with QFF-C, QFF-P200, QFF-P300 and QFF-P500 respectively, while (a) represents the first half of flow-through fraction collected and (b) represents the second half of flow-through fraction collected.

Trillisky *et al.* [89] postulated that the biomolecules with approximately the same size as the pores of the adsorbent can lead to the convective entrapment of biomolecules in the pores. Since the presence of POEGMA polymer on the adsorbent was likely to constrict the pores, an elevated level of protein loss due to the convective entrapment could be expected. Such entrapment within agarose coated adsorbent has also been reported by our previous study [63]. On the other hand, protein trapped within polymer seemed to improve the flow-through recovery of HB-VLPs. The multi-cycle of chromatographic runs of modified adsorbents seemed to reduce the protein loss. For instance, using the adsorbent QFF-P300, the total protein loss in the first, second and third cycle were 16.5%, 15.9%, 13.7% respectively. Therefore, an extensive cyclical test is required to further explore the reusability of the adsorbents.

4.4. Conclusion

From study of Phase 2, the POEGMA-grafted adsorbents were successfully synthesized via free radical graft polymerization approach. The larger-size Q Sepharose FF showed a lower adsorption of HB-VLPs, which is a key factor in achieving a better flow-through recovery. The size-selective properties of POEGMA-grafted adsorbents were qualitatively verified as the protein size of the recovered fraction was found to be larger compared to its ungrafted control. Additionally, POEGMA grafted QFF-P200 effectively reduces disintegration of eluted protein and strongly adsorbed SEC-purified HB-VLPs. When compared to the dextran-grafted QXL-C adsorbent, the inert POEGMA produced a better flow-through recovery of HB-VLPs. Despite the small pore size of QXL-C adsorbents, the additional binding sites on dextran grafts affected the performance of FC. Study of branch-chain length of POEGMA showed that the long-chain $POEGMA_{500}$ produced comparable performance even at a low polymer grafting density. In conclusion, although the modified adsorbent QFF-P300

was able to provide a sufficient exclusion effect for HB-VLPs with flow-through recovery of 92% and PF of 1.53- a 5% improvement of recovery compared to the $POEGMA_{200}$ designed by the previous study. However, a case-by-case tailored adsorbent is required for the exclusion of other target biomolecules of different surface charge density and size.

Chapter 5: General Discussion, Conclusion and Recommendation for the Future Work

5.1. General discussion

Phase 1 aimed to identify suitable feedstock condition (protein load, target protein size) for FC. The results obtained from the comparative study between HB-tridimer and HB-VLP, the capacity of impurities removal with HB-VLPs is significantly reduced (70%), hence, larger amount of adsorbent is needed in the operation with HB-VLP feedstock. The optimum range of protein load of feedstock HB-VLPs for Sepharose Q FF adsorbent was found to be at 30% HCPs breakthrough. The repulsion effect of adsorbed HB-VLPs resulted in a decrease in optimum protein load to 15% HCPs breakthrough or 5.5 mg total protein/ml adsorbent for POEGMA grafted adsorbent. Optimal feedstock condition obtained for polymer modified adsorbent was similar to previous study [14,63]. Compared to feedstock with low purity VLPs such as MrN-VLPs, highly expressed HB-VLPs was more suitable to be purified using FC.

Phase 2 aimed to improve the design of polymer grafted adsorbent for FC. Larger adsorbent was found to provide better flow-through recovery with an offset to purity, while the inert (non-charged) properties of POEGMA was found to be suited for FC applications. OEGMA monomer with longer branch chain length results in POEGMA that is more hydrophilic, producing comparable flow-through recovery and purity despite lower grafted amount. Adsorbent grafted with moderate branch chain length (QFF-P300) was found to provide better (approximately 5%) FC performance compared to short branch chain length (QFF-P200) of previous study by our research group [63].

5.2. Conclusion

For the initial isolation step of HB-VLPs from its clarified *E. coli* homogenate, the current study successfully identified suitable condition of feedstock in the FC mode using POEGMA grafted cationized adsorbent. The optimal condition is at 5.5 mg total protein/ml of adsorbent. While the 2nd phase established standard size diffusive adsorbents grafted with moderate branch chain (QFF-P300) as the optimal adsorbent design suitable for the intended application. Compared to the previous study, slight improvement in flow-through recovery of HB-VLPs was achieved with longer branch chain length $POEGMA_{300}$ – with a flow-through recovery of 92% and PF of 1.53. Further work are recommended to improve the performance of the adsorbents as well as establish a platform for the VLP purification.

5.3. Recommendations for future work

The feedstock condition can be improved further for FC operation. The amount of residual DNA can be measured and treated with nucleases prior to chromatography. Since the size of DNAs are similar to HB-VLPs [59], and are likely to be excluded along with the target protein. Addition of nucleases could reduce the size of DNA and improve its adsorption and removal. Besides, large HCPs was observed in the flowthrough fractions. Adding an ultra/diafiltration step before the negative chromatography could help to eliminate the impurities before the negative chromatography. However, the cost of the additional step should be taken into account.

The design of the adsorbent can also be improved further. For instance, the grafting density can be improved by adopting other grafting reaction or technique. Atom transfer radical polymerization (ATRP) from immobilized initiators otherwise known as ‘Grafting from’ techniques allow precise control over grafting density [98]. This would in turn allow better control of the size selective properties i.e. a more defined molecular weight cut-off that would in turn improve applicability for different feedstock. Extensive cyclical test should be conducted to establish the reusability of the POEGMA grafted adsorbents as protein entrapment was found to be an issue.

References

[1] Pumpens, P., Grens, E., HBV core particles as a carrier for B cell / T cell epitopes. *Intervirology* 2001, 1067, 98–114.

[2] Wolf, M. W., Reichl, U., Downstream processing of cell culture-derived virus particles. *Expert Rev. Vaccines* 2011, 10, 1451–1475.

[3] Rolland, D., Gauthier, M., Dugua, J. M., Fournier, C., Delpech, L., Watelet, B., Letourneur, O., Arnaud, M., Jolivet, M., Purification of recombinant HBc antigen expressed in *Escherichia coli* and *Pichia pastoris*: Comparison of size-exclusion chromatography and ultracentrifugation. *J. Chromatogr. B Biomed. Sci. Appl.* 2001, 753, 51–65.

[4] Ng, M. Y. T., Tan, W. S., Abdullah, N., Ling, T. C., Tey, B. T., Direct purification of recombinant hepatitis B core antigen from two different pre-conditioned unclarified *Escherichia coli* feedstocks via expanded bed adsorption chromatography. *J. Chromatogr. A* 2007, 1172, 47–56.

[5] Yu, M., Li, Y., Zhang, S., Li, X., Yang, Y., Chen, Y., Ma, G., Su, Z., Improving stability of virus-like particles by ion-exchange chromatographic supports with large pore size: Advantages of gigaporous media beyond enhanced binding capacity. *J. Chromatogr. A* 2014, 1331, 69–79.

[6] DePhillips, P., Lenhoff, A. M., Pore size distributions of cation-exchange adsorbents determined by inverse size-exclusion chromatography. *J. Chromatogr. A* 2000, 883, 39–54.

[7] Gagnon, P., The emerging generation of chromatography tools for virus purification. *Bioprocess Int.* 2008, 6, Suppl. 6 24-30.

[8] Wu, Y., Abraham, D., Carta, G., Particle size effects on protein and virus-like particle adsorption on perfusion chromatography media. *J. Chromatogr. A* 2015, 1375, 92–100.

[9] Wu, Y., Simons, J., Hooson, S., Abraham, D., Carta, G., Protein and virus-like particle adsorption on perfusion chromatography media. *J. Chromatogr. A* 2013, 1297, 96–105.

[10] Weigel, T., Solomaier, T., Peuker, A., Pathapati, T., Wolff, M. W., Reichl, U., A flow-through chromatography process for influenza A and B virus purification. *J. Virol. Methods* 2014, 207, 45–53.

[11] Wang, C., Soice, N. P., Ramaswamy, S., Gagnon, B. A., Umana, J., Cotoni, K. A., Bian, N., Cheng, K.-S. C., Cored anion-exchange chromatography media for antibody flow-through purification. *J. Chromatogr. A* 2007, 1155, 74–84.

[12] Blom, H., Åkerblom, A., Kon, T., Shaker, S., Pol, L. Van Der, Lundgren, M., Efficient chromatographic reduction of ovalbumin for egg-based influenza virus purification. *Vaccine* 2014, 32, 3721–3724.

[13] Yoon, K. Y., Tan, W. S., Lee, K. W., Ho, K. L., Native agarose gel electrophoresis and electroelution : A fast and cost-effective method to separate the small and large hepatitis B capsids. *Electrophoresis* 2013, 34, 244–253.

[14] Lee, M. F. X., Chan, E. S., Tan, W. S., Tam, K. C., Tey, B. T., Negative chromatography purification of hepatitis B virus-like particles using poly(oligo(ethylene glycol) methacrylate) grafted cationic adsorbent. *J. Chromatogr. A* 2015, 1415, 161–165.

[15] Zeltins, A., Construction and characterization of virus-like particles: A review. *Mol.*

Biotechnol. 2013, 53, 92–107.

[16] Shirbaghaee, Z., Bolhassani, A., Different applications of virus-like particles in biology and medicine: Vaccination and delivery systems. *Biopolymers* 2016, 105, 113–132.

[17] Roldao, A., Mellado, M. C. M., Castilho, L. R., Carrondo, M. J., Alves, P. M., Virus-like particles in vaccine development. *Expert Rev. Vaccines* 2010, 9, 1149–1176.

[18] Lua, L. H. L., Connors, N. K., Sainsbury, F., Chuan, Y. P., Wibowo, N., Middelberg, A. P. J., Bioengineering virus-like particles as vaccines. *Biotechnol. Bioeng.* 2014, 111, 425–440.

[19] Huang, Y., Bi, J., Zhou, W., Li, Y., Wang, Y., Ma, G., Su, Z., Improving recovery of recombinant hepatitis B virus surface antigen by ion-exchange chromatographic supports with low ligand density. *Process Biochem.* 2006, 41, 2320–2326.

[20] Vanlandschoot, P., Cao, T., Leroux-roels, G., The nucleocapsid of the hepatitis B virus : a remarkable immunogenic structure. *Antiviral Res.* 2003, 60, 67–74.

[21] Schodel, F., Peterson, D., Milich, D., Hepatitis B virus core and e antigen: immune recognition and use as a vaccine carrier moiety. *Intervirology* 1996, 39, 104–110.

[22] Elvidge, S., Blockbuster expectations for hepatitis B therapeutic vaccine. *Nat. Biotechnol.* 2015, 789.

[23] Morenweiser, R., Downstream processing of viral vectors and vaccines. *Gene Ther.* 2005, 12 Suppl 1, S103-10.

[24] Palenzuela, D. O., Núñez, L., Roca, J., Acevedo, B., Díaz, T., Benítez, J., Gavilondo, J. V, Purification of the recombinant hepatitis B core antigen, and its potential use for the diagnosis of Hepatitis B virus infection. *Biotecnol. Apl.* 2002, 19, 138–142.

[25] Ng, M. Y. T., Tan, W. S., Abdullah, N., Ling, T. C., Tey, B. T., Heat treatment of unclarified *Escherichia coli* homogenate improved the recovery efficiency of recombinant hepatitis B core antigen. *J. Virol. Methods* 2006, 137, 134–139.

[26] Wolff, M. W., Reichl, U., Downstream processing: From egg to cell culture-derived influenza virus particles. *Chem. Eng. Technol.* 2008, 31, 846–857.

[27] Carta, G., Jungbauer, A., Protein Chromatography. 2010, pp. 85–124.

[28] Wu, Y., Simons, J., Hooson, S., Abraham, D., Carta, G., Protein and virus-like particle adsorption on perfusion chromatography media. *J. Chromatogr. A* 2013, 1297, 96–105.

[29] Sviben, D., Forcic, D., Ivancic-Jelecki, J., Halassy, B., Brgles, M., Recovery of infective virus particles in ion-exchange and hydrophobic interaction monolith chromatography is influenced by particle charge and total-to-infective particle ratio. *J. Chromatogr. B Anal. Technol. Biomed. Life Sci.* 2017, 1054, 10–19.

[30] Yang, Y., Mengran Yu, Zhang, S., Ma, G., Su, Z., Adsorption of virus-like particles on ion exchange surface: Conformational changes at different pH detected by dual polarization interferometry. *J. Chromatogr. A* 2015, 1408, 161–168.

[31] Iyer, G., Ramaswamy, S., Asher, D., Mehta, U., Leahy, A., Chung, F., Cheng, K.-S., Reduced surface area chromatography for flow-through purification of viruses and virus like particles. *J. Chromatogr. A* 2011, 1218, 3973–81.

[32] Huang, Y., Bi, J., Zhao, L., Ma, G., Su, Z., Regulation of protein multipoint adsorption on ion-exchange adsorbent and its application to the purification of macromolecules. *Protein Expr. Purif.* 2010, 74, 257–63.

[33] Lu, X., Zhao, D., Ma, G., Su, Z., Polyethylene glycol increases purification and

recovery , alters retention behavior in flow-through chromatography of hemoglobin. *J. Chromatogr. A* 2004, 1059, 233–237.

[34] Wang, Y., Zhang, P., Liu, S., Zhang, Y., Zhao, T., Huang, W., He, C., Yu, Y., Wang, L., Wan, M., Purification of IgG from sera of rabbit and guinea pig by flow-through mode ion-exchange chromatography using DEAE sepharose fast flow column. *Chromatographia* 2011, 74, 209–214.

[35] Burbelo, P., Kisailus, A., Peck, J. W., Negative purification method for the selection of specific antibodies from polyclonal antisera. *Biotechniques* 2002, 33, 1050–1054.

[36] Bjerke, T., Nielsen, S., Helgestad, J., Nielsen, B. W., Purification of human blood basophils by negative selection using immunomagnetic beads. *J. Immunol. Methods* 1993, 157, 49–56.

[37] Neale, A. D., Scopes, R. K., Kelly, J. M., Wettenhall, E. H., The two alcohol dehydrogenases of Zymomonas mobilis and physiological roles. *Eur. J. Biochem.* 1986, 154, 119–124.

[38] Hey, Y., Dean, P. D., Tandem dye-ligand chromatography and biospecific elution applied to the purification of glucose-6-phosphate dehydrogenase from Leuconostoc mesenteroides. *Biochem. J.* 1983, 209, 363–371.

[39] Scopes, R. K., Griffiths-Smith, K., Use of differential dye-ligand chromatography with affinity elution for enzyme purification: 6-Phosphogluconate dehydratase from Zymomonas mobilis. *Anal. Biochem.* 1984, 136, 530–534.

[40] Pitiot, O., Nedonchelle, E., Vijayalakshmi, M. A., Protein adsorption on histidyl-aminohexyl-Sepharose 4B II . Application to the negative one-step affinity purification of human b 2-microglobulin and Immunoglobulin G. 2001, 758, 173–182.

[41] Cristiane, M., Souza, M. De, Tadeu, I., Bresolin, L., Maria, S., Bueno, A., Purification of human IgG by negative chromatography on ω-aminohexyl-agarose. *J. Chromatogr. B* 2010, 878, 557–566.

[42] Bresolin, I. T. L., de Souza, M. C. M., Bueno, S. M. A., A new process of IgG purification by negative chromatography: Adsorption aspects of human serum proteins onto α-aminodecyl-agarose. *J. Chromatogr. B Anal. Technol. Biomed. Life Sci.* 2010, 878, 2087–2093.

[43] Bresolin, I. ., Fioritti, R., Bueno, S., IgG purification by negative chromatography in amine-based ligands : A comparison of l -lysine and poly- l -lysine. *Process Biochem.* 2011, 46, 2277–2285.

[44] Brooks, S. P., Storey, K. B., Purification and characterization of a protein phosphatase that dephosphorylates pyruvate kinase in an anoxia tolerant animal. *Biochem. Mol. Biol. Int.* 1996, 38, 1223–34.

[45] Lu, X., Zhao, D., Su, Z., Purification of hemoglobin by ion exchange chromatography in flow-through mode with PEG as an escort purification of hemoglobin by ion exchange. *Artif. Cells, Blood Substitutes, Biotechnol.* 2009, 32, 209–227.

[46] Wongchuphan, R., Tey, T., Siang, W., Kumar, S., Saleena, F., Chuan, T., Purification of rabbit polyclonal immunoglobulin G using anion exchangers. *Process Biochem.* 2011, 46, 101–107.

[47] Champion, K. M., Nishihara, J. C., Joly, J. C., Arnott, D., Similarity of the *Escherichia coli* proteome upon completion of different biopharmaceutical fermentation processes. *Proteomics* 2001, 1, 1133–1148.

[48] Zheng, J., Schodel, F., Peterson, D. L., The structure of hepadnaviral core antigens.

Identification of free thiols and determination of the disulfide bonding pattern. *J. Biol. Chem.* 1992, 267, 9422–9429.

[49] Yoshida, H., Morita, I., Tamai, G., Masujima, T., Tsuru, T., Takai, N., Imai, H., Some characteristics of a protein-coated ODS column and its use for the determination of drugs by the direct injection analysis of plasma samples. *Chromatographia* 1984, 19, 466–472.

[50] Souverain, S., Rudaz, S., Veuthey, J. L., Restricted access materials and large particle supports for on-line sample preparation: An attractive approach for biological fluids analysis. *J. Chromatogr. B Anal. Technol. Biomed. Life Sci.* 2004, 801, 141–156.

[51] Cassiano, N. M., Lima, V. V., Oliveira, R. V., De Pietro, A. C., Cass, Q. B., Development of restricted-access media supports and their application to the direct analysis of biological fluid samples via high-performance liquid chromatography. *Anal. Bioanal. Chem.* 2006, 384, 1462–1469.

[52] Yang, S. H., Fan, H., Classon, R. J., Schug, K. A., Restricted access media as a streamlined approach toward on-line sample preparation: Recent advancements and applications. *J. Sep. Sci.* 2013, 36, 2922–2938.

[53] Kanda, T., Kutsuna, H., Ohtsu, Y., Yamaguchi, M., Synthesis of polymer-coated mixed-functional packing materials for direct analysis of drug-containing serum and plasma by high-performance liquid chromatography. *J. Chromatogr. A* 1994, 672, 51–57.

[54] Katagi, M., Nishikawa, M., Tatsuno, M., Miki, A., Tsuchihashi, H., Column-switching high-performance liquid chromatography-electrospray ionization mass spectrometry for identification of heroin metabolites in human urine. *J. Chromatogr. B Biomed. Sci. Appl.* 2001, 751, 177–185.

[55] Tian, R., Zhang, H., Ye, M., Jiang, X., Hu, L., Li, X., Bao, X., Zou, H., Selective extraction of peptides from human plasma by highly ordered mesoporous silica particles for peptidome analysis. *Angew Chem Int Ed Engl* 2007, 46, 962–965.

[56] Hu, L., Zhou, H., Li, Y., Sun, S., Guo, L., Ye, M., Tian, X., Gu, J., Yang, S., Zou, H., Profiling of endogenous serum phosphorylated peptides by titanium (IV) immobilized mesoporous silica particles enrichment and MALDI-TOFMS detection. *Anal. Chem.* 2009, 81, 94–104.

[57] Jahanshahi, M., Zhang, Z., Lyddiatt, A., Subtractive chromatography for purification and recovery of nano-bioproducts. *IEEE Proc. nanobiotechnology* 2005, 152, 207–211.

[58] Jahanshahi, M., Aghajani, H., Ling, T., Assembly and purification of nanostructure bioproducts: Protein nanoparticle characterization and non-stick exterior coating adsorbents. *Int. J. Nanosci. Nanotechnol* 2005, 1, 9–20.

[59] Gustavsson, P., Lemmens, R., Nyhammar, T., Busson, P., Larsson, P., Purification of plasmid DNA with a new type of anion-exchange beads having a non-charged surface. *J. Chromatogr. A* 2004, 1038, 131–140.

[60] GE Healthcare, L. S., GE Healthcare Life Sciences "Q and SP Sepharose™ Big Beads."

[61] GE Healthcare, L. S., GE Healthcare Life Sciences "Capto™ Core 700."

[62] Nestola, P., Peixoto, C., Villain, L., Alves, P. M., Carrondo, M. J. T., Mota, P. B., Rational development of flow-through purification strategies for viruses and virus-like particles. *J. Chromatogr. A* 2015, 1426, 1–39.

[63] Lee, M. F. X., Chan, E. S., Tan, W. S., Tam, K. C., Tey, B. T., Negative

chromatography of hepatitis B virus-like particle: Comparative study of different adsorbent designs. *J. Chromatogr. A* 2016, 1445, 1–9.

[64] Lee, M. F. X., Chan, E. S., Tan, W. S., Tam, K. C., Tey, B. T., Negative chromatography purification of hepatitis B virus-like particles using poly(oligo(ethylene glycol) methacrylate) grafted cationic adsorbent. *J. Chromatogr. A* 2015, 1415, 161–165.

[65] Jeon, S. ., Lee, J. ., Andrade, J. ., De Gennes, P. ., Protein—surface interactions in the presence of polyethylene oxide. *J. Colloid Interface Sci.* 1991, 142, 149–158.

[66] Lowe, S., O'Brien-Simpson, N. M., Connal, L. A., Antibiofouling polymer interfaces: poly(ethylene glycol) and other promising candidates. *Polym. Chem.* 2015, 6, 198–212.

[67] Heuberger, M., Drobek, T., Spencer, N. D., Interaction forces and morphology of a protein-resistant poly(ethylene glycol) layer. *Biophys. J.* 2005, 88, 495–504.

[68] Chan, Y. H. M., Schweiss, R., Werner, C., Grunze, M., Electrokinetic characterization of oligo- and poly(ethylene glycol)-terminated self-assembled monolayers on gold and glass surfaces. *Langmuir* 2003, 19, 7380–7385.

[69] Szleifer, I., Protein adsorption on tethered polymer layers: effect of polymer chain architecture and composition. *Phys. A Stat. Mech. its Appl.* 1997, 244, 370–388.

[70] Hucknall, A., Rangarajan, S., Chilkoti, A., In Pursuit of Zero: Polymer Brushes that Resist the Adsorption of Proteins. *Adv. Mater.* 2009, 21, 2441–2446.

[71] Tsukagoshi, T., Kondo, Y., Yoshino, N., Protein adsorption on polymer-modified silica particle surface. *Colloids Surfaces B Biointerfaces* 2007, 54, 101–107.

[72] Yoshikawa, C., Goto, A., Ishizuka, N., Nakanishi, K. K., Kishida, A., Tsujii, Y.,

Fukuda, T., Radical Polymerization: Kinetics and Mechanism. WILEY-VCH Verlag 2007, pp. 189–198.

[73] Brooks, D. E., Haynes, C. A., Hritcu, D., Steels, B. M., Müller, W., Size exclusion chromatography does not require pores. *Proc. Natl. Acad. Sci. U. S. A.* 2000, 97, 7064–7.

[74] Gunkel, G., Weinhart, M., Becherer, T., Haag, R., Huck, W. T. S., Effect of polymer brush architecture on antibiofouling properties. *Biomacromolecules* 2011, 12, 4169–4172.

[75] Tey, B. T., Yong, K. H., Ong, H. P., Ling, T. C., Ong, S. T., Tan, Y. P., Ariff, A., Tan, W. S., Optimal conditions for hepatitis B core antigen production in shaked flask fermentation. *Biotechnol. Bioprocess Eng.* 2004, 9, 374–378.

[76] Watelet, B., Quibriac, M., Rolland, D., Gervasi, G., Gauthier, M., Jolivet, M., Letourneur, O., Erratum to ‘‘ Characterization and diagnostic potential of hepatitis B virus nucleocapsid expressed in E. coli and P. pastoris". *J. Virol. Methods* 2002, 102, 7887.

[77] Yap, W. B., Tey, B. T., Alitheen, N. B. M., Tan, W. S., Purification of His-tagged hepatitis B core antigen from unclarified bacterial homogenate using immobilized metal affinity-expanded bed adsorption chromatography. *J. Chromatogr. A* 2010, 1217, 3473–3480.

[78] Ng, M. Y. T., Siang, W., Tey, T., Purification of recombinant hepatitis B core antigen from unclarified *Escherichia coli* feedstock using phage-immobilized expanded bed adsorption chromatography. *J. Chromatogr. B* 2012, 903, 60–67.

[79] Ho, C. W., Tan, W. S., Kamaruddin, S., Ling, T. C., Tey, B. T., The direct recovery of

recombinant hepatitis B core antigen from disruptate derived from continuous-flow bead milling. *Biotechnol. Appl. Biochem.* 2008, 50, 49–59.

[80] Vennapusa, R., Hunegnaw, S. M., Cabrera, R. B., Fernández-Lahore, M., Assessing adsorbent-biomass interactions during expanded bed adsorption onto ion exchangers utilizing surface energetics. *J. Chromatogr. A* 2008, 1181, 9–20.

[81] Lee, K. W., Tey, B. T., Ho, K. L., Tejo, B. A., Tan, W. S., Nanoglue: An alternative way to display cell-internalizing peptide at the spikes of Hepatitis B virus core nanoparticles for cell-targeting delivery. *Mol. Pharm.* 2012, 9, 2415–2423.

[82] Yoon, K. Y., Expression, Purification and Structural Characterisation of Hepatitis B Virus Core Antigen with an N-Terminal Extension, Universiti Putra Malaysia, 2013.

[83] Zhu, M., Carta, G., Adsorption of polyethylene-glycolated bovine serum albumin on macroporous and polymer-grafted anion exchangers. *J. Chromatogr. A* 2014, 1326, 29–38.

[84] Liu, H. F., McCooey, B., Duarte, T., Myers, D. E., Hudson, T., Amanullah, A., van Reis, R., Kelley, B. D., Exploration of overloaded cation exchange chromatography for monoclonal antibody purification. *J. Chromatogr. A* 2011, 1218, 6943–6952.

[85] Lee, M. F. X., Chan, E. S., Tam, K. C., Tey, B. T., Thermo-responsive adsorbent for size-selective protein adsorption. *J. Chromatogr. A* 2015, 1394, 71–80.

[86] Bradford, M. M., A rapid and sensitive method for the quantitation of microgram quantities of protein utilizing the principle of protein-dye binding. *Anal. Biochem.* 1976, 72, 248–254.

[87] Laemmli, U. K., Cleavage of structural proteins during the assembly of the head of bacteriophage T4. *Nature* 1970, 227, 680–685.

[88] Sigma-Aldrich, Fluorescein Isothiocyanate.

[89] Trilisky, E. I., Lenhoff, A. M., Flow-dependent entrapment of large bioparticles in porous process media. *Biotechnol. Bioeng.* 2009, 104, 127–133.

[90] Yong, C. Y., Yeap, S. K., Goh, Z. H., Ho, K. L., Omar, A. R., Tan, W. S., Induction of humoral and cell-mediated immune responses by hepatitis B virus epitope displayed on the virus-like particles of prawn nodavirus. *Appl. Environ. Microbiol.* 2015, 81, 882–889.

[91] Kalbfuss, B., Wolff, M., Morenweiser, R., Reichl, U., Purification of cell culture-derived Human Influenza A virus by size-exclusion and anion-exchange chromatography. *Biotechnol. Bioeng.* 2006, 96, 932–944.

[92] Lyddiatt, A., O'Sullivan, D. A., Biochemical recovery and purification of gene therapy vectors. *Curr. Opin. Biotechnol.* 1998, 9, 177–185.

[93] Lenhoff, A. M., Protein adsorption and transport in polymer-functionalized ion-exchangers. *J. Chromatogr. A* 2011, 1218, 8748–8759.

[94] Yao, Y., Lenhoff, A. M., Pore size distributions of ion exchangers and relation to protein binding capacity. *J. Chromatogr. A* 2006, 1126, 107–119.

[95] Biosciences, A., Q Sepharose Fast Flow Product Data. n.d.

[96] GE Healthcare, L. S., Q Sepharose High Performance Product Data (Data File 18-1172-88 AB). n.d.

[97] Bowes, B. D., Koku, H., Czymmek, K. J., Lenhoff, A. M., Protein adsorption and transport in dextran-modified ion-exchange media . I : Adsorption. *J. Chromatogr. A* 2009, 1216, 7774–7784.

[98] Nagase, K., Kobayashi, J., Kikuchi, A., Akiyama, Y., Kanazawa, H., Okano, T., Effects of graft densities and chain lengths on separation of bioactive compounds by nanolayered thermoresponsive polymer brush surfaces. *Langmuir* 2008, 24, 511–7.